Spring 4-14-2017

HYPORHEIC NITRATE UPTAKE AND STOICHIOMETRIC LIMITATIONS: MESOCOSM EXPERIMENTS ALONG A RIVER CONTINUUM.

Vanessa A. Garayburu Caruso

Vanessa Garayburu-Caruso
Candidate

Department of Civil Engineering
Department

This thesis is approved, and it is acceptable in quality and form for publication:

Approved by the Thesis Committee:

Ricardo González-Pinzón PhD, Chairperson

David Van Horn PhD.

Tim Covino PhD.

Jose Cerrato PhD.

HYPORHEIC NITRATE UPTAKE AND STOICHIOMETRIC LIMITATIONS: MESOCOSM EXPERIMENTS ALONG A RIVER CONTINUUM.

by

VANESSA A. GARAYBURU-CARUSO

B.S. CHEMICAL ENGINEERING 2014
UNIVERSIDAD SIMON BOLIVAR, CARACAS VENEZUELA

THESIS

Submitted in Partial Fulfillment of the
Requirements for the Degree of

Master of Science
Civil Engineering

The University of New Mexico
Albuquerque, New Mexico

May, 2017

DEDICATION

A Dios y a mi familia, por su amor incondicional, su apoyo, por siempre motivarme y creer en mi. Todos mis logros se los debo a ustedes, gracias por enseñarme a seguir mis sueños y nunca rendirme.

ACKNOWLEDMENTS

I would like to thank Dr. González-Pinzón, my advisor and committee chairperson, for this amazing opportunity, his experience, guidance, support and his friendship. Your advices and mentorship have helped me to grow as a person and as a researcher. Thank you for this amazing journey and all the great learning experiences.

I would also like to acknowledge Dr. Van Horn for your input and guidance. Thanks for helping me improve the interdisciplinary aspects of this study. I want to acknowledge my committee member, Dr. Covino, for your guidance and invaluable insights on nutrient metrics. Thank you to Dr. Cerrato for your guidance, mentorship, friendship and unconditional support. Thanks to all my committee for your time and feedback.

I also want to express my gratitude to all the professors who have helped me look at science with a different pair of eyes. My time at UNM has been academically enriching and fulfilling.

Finally, I would like to thank my family for always being there for me, even in the distance, and my friends for becoming the best second family I could ever ask for. Thanks for your love and support.

HYPORHEIC NITRATE UPTAKE AND STOICHIOMETRIC LIMITATIONS: MESOCOSM EXPERIMENTS ALONG A RIVER CONTINUUM.

by

Vanessa A. Garayburu-Caruso

B.S. in Chemical Engineering, Universidad Simon Bolivar, 2014

M.S. Civil Engineering, University of New Mexico, 2017

ABSTRACT

Nutrient uptake in streams and rivers is controlled by complex transport dynamics and biogeochemical interactions, which together regulate nutrient export from watersheds. Decoupling the relative contributions of transport and biogeochemical processes to nutrient uptake at the watershed scale has been challenging due to the spatial and temporal heterogeneity of physicochemical properties. Furthermore, logistical constraints have resulted in solute-specific analyses, primarily concentrated in headwater streams, that disregard the role of stoichiometry in controlling biological uptake. We used experimental mesocosm (column experiments) along the Jemez River-Rio Grande continuum (1^{st}-8^{th} stream order) to isolate spatial differences in biological nitrate uptake. Columns were constructed out of PVC, packed with gravel, silica sand and native sediments, and colonized *in-situ* for three months to allow the establishment of native microbial communities from each stream order. After incubation, we conducted two sets

of tracer additions in each column under uniform flow conditions to analyze nitrate uptake for nitrate only injections and for stoichiometrically 'balanced' (106C:16N:1P) resource supply injections (i.e., nitrate vs Redfield experiments). We quantified NO_3-N uptake kinetics using the TASCC method. We observed higher ranges of NO_3-N uptake velocities (V_{f-add}) relative to concentration during Redfield experiments. Highest nitrate uptake was observed in 7th order mesocosms packed with native sediments ($V_{f-median}$ = 0.05 mm min^{-1}). Nitrate kinetics predominantly followed Michaelis-Menten patterns. The comparison of the two injection experiments suggested that biological NO_3-N processing was generally co-limited and the limitation varied with stream order and type of substrate. Our results support the notion that natural stoichiometric imbalances limit nutrient uptake in lotic systems and may explain the lack of scaling patterns observed in solute-specific nutrient uptake analyses.

LIST OF FIGURES

LIST OF TABLES

TABLE OF CONTENTS

INTRODUCTION

In-stream processes control nutrient retention (biological uptake and storage) and thus mitigate exports from terrestrial landscapes to downstream ecosystems (Alexander et al. 2000; Bernhart et al. 2003). The benthic and hyporheic zones in streams are critical to this retention of nutrients, but their contribution to aquatic nutrient budgets vary in space and time (Hendricks 1993; Poole et al., 2008; Pinay et al., 2009; Boano et al., 2010; Marzadri et al., 2011; Wondzell, 2011; Zarnetske et al., 2011a; Bardini et al., 2012; Mortensen et al., 2016; Knapp et al., 2017). Nutrient uptake is controlled by transport dynamics (i.e., advection, dispersion, transient storage) and biogeochemical interactions of nutrients in metabolically active zones. Transport to benthic and hyporheic zones depends on hydrologic and physical processes (i.e., discharge, pressure gradients, hydraulic conductivity, channel geomorphology, topography and fine sediment transport), while biogeochemical interactions depend on nutrient availability, redox conditions, dissolved organic matter, pH, temperature and spatial heterogeneity of bacterial diversity (Zarnetske et al., 2012; Zeglin, 2015; Gonzalez-Pinzon et al., 2015; Knapp et al., 2017).

Despite considerable research done to understand in-stream nutrient uptake (Ensign and Doyle, 2006; Mulholland et al., 2008; Tank et al., 2008; Mulholland et al., 2009; Hall et al., 2013), most studies have focused on site-specific (Hill et al., 2010; Figueroa-Nieves et al., 2015) and solute-specific analyses (Newbold et al., 1983; Mulholland et al., 2002; Dodds et al., 2002; Hall et al., 2013; Wollheim et al., 2014; Trentman et al., 2015). Site-specific analyses have largely explored local (i.e., lateral sand bars, upwelling and downwelling zones) and reach (typically < 1000 m long) scales. In doing so, most work

reported to date has quantified nutrient uptake using either: 1) lumped transport models (fast moving main channel vs. slow moving benthic and hyporheic zones), thus only considering the bulk influence of flow and apparent transport parameters (resulting from the homogenization of the suite of metabolically active zones) to inform rates of nutrient retention; or 2) residence time distribution analyses seeking to correlate nutrient exposure times for biofilm and macrophyte uptake with bulk nutrient retention (informed by mass balances) (Valett et al., 1996; Hall et al., 2002; Gomez et al., 2012; Kiel and Cardenas, 2014; Zarnetske et al., 2012). Since most nutrient uptake experiments have focused on understanding the uptake of one nutrient at a time (e.g., only nitrogen or only phosphorous), most experimental evidence has neglected stoichiometric constraints known to control nutrient uptake at the cellular scale (Redfield, 1958; Hecky et al., 1993; Klausmeier et al., 2004). Therefore, largely unexplored variations in the availability of key macronutrients may limit the cycling of other nutrients at the reach and watershed scales (Elser et al. 2009; Marklein and Houlton 2012; Appling and Heffernan 2014). To date, the concepts of nutrient limitation and colimitation in freshwater systems have been explored by ecologists (e.g., Francoeur 2001; Elser et al., 2007; Allgeier et al., 2011; Harpole et al., 2011), but only a few studies have attempted to test these controls at the reach or watershed scales (e.g. Brookshire et al., 2005; Schade et al., 2011; Gibson and O'Reilly 2012; Cohen et al., 2013; Rodriguez-Cardona et al. 2015, Piper et al., 2017). Consequently, we still lack an understanding of how natural and anthropogenically modifed nutrient supply (most likely stroichiometrically imbalanced) controls nutrient uptake across watersheds (Fisher et al. 2004; Hall et al., 2009).

In this manuscript, we explore stoichiometric controls on hyporheic nitrate uptake across an arid land watershed. Our approach departs from the status quo in three ways: 1) we depart from site-specific analyses and present experimental results from representative sites across 1st – 8th order streams; 2) we depart from solute-specific nutrient uptake analyses and present multi-site results for nitrate uptake under a) nitrate tracer additions, and b) 106:16:1 (C:N:P) ratios; and 3) we used consistent and reproducible experimental techniques for all of our experiments, which is a goal that only a handful of nutrient experimental programs (e.g. LINXs I and II; Webster et al., 2003; Payn et al., 2005; Mulholand et al., 2008) have explicitly targeted. The specific objectives of this study were to: 1) compare the efficiency of nitrate processing in riverbed sediments using naturally occurring sediments from different sites along the continuum and commercially available artificial substrates, 2) assess potential saturation of biological nitrate consumption using functional relationships between nutrient uptake and concentration (kinetic models), and 3) study the efficiency of nitrate removal under stoichiometrically variable C:N:P nutrient supply. Our mesocosm experiments suggest that stoichiometric limitations influence nitrate uptake along the river continuum based on the initial nutrient limitation of the system.

MATERIALS AND METHODS

Site Description

We conducted column experiments using sediments from sites along a ~300 km river continuum formed by the Jemez River (1st-5th order streams; ~98.5 km) and the Rio Grande (7th-8th order streams; ~290 km) in New Mexico, USA. The headwaters of the

Jemez River (1st to 3rd order streams) are in the Valles Caldera National Preserve (co-located with the Jemez-Catalina CZO). The vegetation within the catchment is composed primarily by montane riparian grassland (Parmenter et al., 2007). The Jemez River becomes a 4th order stream after the confluence with the San Antonio River, where the stream receives geothermal inflows from fractures associated with the Jemez Fault. After the confluence with the Rio Guadalupe, the Jemez River flows as a 5th order stream until it connects with the Rio Grande. Riparian vegetation along the Jemez River is composed of alder, willow, cottonwood, cattail (*Typha spp*.), sedges, reeds, juncus (*Juncus spp.)* and grasses (Tetra Tech, INC, 2005). The geology is dominated by volcanic rock formations in the headwaters and by quaternary valley-fill alluvium, terrace-gravel deposits, travertine deposits and sandstone and shale beds (Craigg, 1992). Activities associated to ranching, irrigated and dry-land agriculture, and recreation take place in this area.

The Rio Grande section (7th and 8th order streams) is from the City of Bernalillo to Elephant Butte Reservoir. The Rio Grande as a 7th order river runs through urban centers in central NM, where four WWTPs (Bernalillo, Rio Rancho, Albuquerque, and Los Lunas) discharge into its waters. The Albuquerque Southside Reclamation Plant is the most significant source of nutrients to the river, discharging an estimated load of 980 kg day^{-1} of dissolved inorganic nitrogen at an average flow rate of 2.3 m^3 s^{-1} (Passel et al., 2005; Oelsner et al., 2007; Mortensen et al., 2016). During its course, the river is controlled by dams and is diverted for agriculture and water supply (Reale et al., 2015; Dahm et al., 2015). The Rio Grande becomes an 8th order stream after the confluence with the Rio Puerco and remains as 8th order stream until it discharges into the Gulf of Mexico. The flood plain of this area is comprised predominantly of cottonwood (*Populus*

Fremontii), willow (*Salix spp.*), Russian-olive (*Elaeagnus angustifolia*), and salt cedar (*Tamariz chinensis*), mixed with pasture and cultivated land (Lagasse 1981). The Rio Grande Basin lies in the Rio Grande rift valley, formed more than 25 million years ago. The geology of this area is a combination of sediment deposits from mountain front alluvial fans, rivers and streams, or sand dunes (Bartolino and Cole, 2002).

We sampled one representative site for each stream order along the Jemez River-Rio Grande Continuum (Figure 1) to perform our mesocosm experiments. Additionally, in the 7^{th} order stream, we sampled upstream and downstream of the Albuquerque Southside Reclamation Plant (7^{th}_A and 7^{th}_B sites, respectively) to analyze the effects of wastewater effluent discharges on nutrient uptake. Along the continuum, the stream-bed sediments varied from coarse sand, gravel and pebbles in headwater sites to very fine sand and silty clay at downstream reaches. Watershed area, discharge ranges, and sediment characteristics for each site are reported in (Table 1). Ambient surface water nitrogen (N) and phosphorous (P) concentrations taken from each study site are presented in Table 2.

Mescosom Setup

Our mesocosm design for each study site consisted on six PVC cylindrical columns with length and diameter dimensions of 0.5 m and 0.05 m, respectively. The columns were packed in two replicates with three different materials: 1) silica cone density sand ASTM D 1556 (0.075-2.00 mm), 2) commercial gravel (2–4 mm) and 3) native sediments. The different packing materials were selected to explore the (post-incubation) variability in nutrient processing associated with sediment texture and colonization by native sediment bacterial communities versus communities being transported in the water column. The

columns filled with native substrate were packed at the site using sediments from the channel thalweg, when possible (1st to 5th order streams), and from near the banks when high flows prevented safely accessing the thalweg (7th-8th order streams).

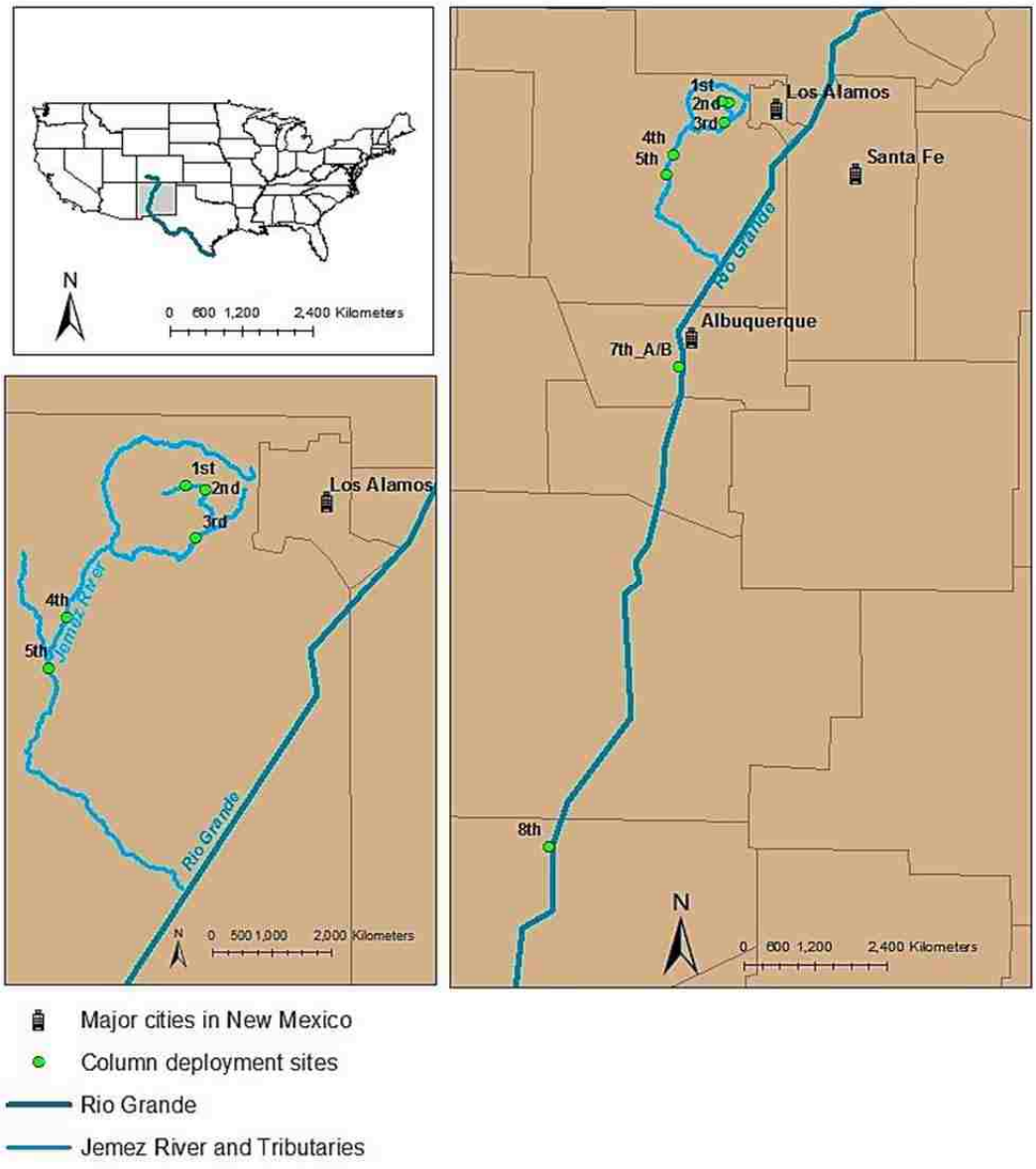

Figure 1. (a) New Mexico (NM), USA. (b) Study sites on the Jemez River (~98.5 km) and the Rio Grande (~290 km) continuum. (c) Study sites along the Jemez River continuum (Jemez River and Jaramillo Creek).

Table 1. Study sites characteristics along the Jemez-Rio Grande Continuum. *Average measured discharge during late spring and summer months in 2015 and 2016. **Min-max (daily average) discharge based on 62 years of USGS records.

Site	Watershed Area (Km^2)	Q (L/s)	Stream-bed characteristics
1st order	5	56*	Cobble/bedrock
2nd order	27	61*	Cobble/bedrock
3rd order	155	298*	Cobble/gravel
4th order	511	509*	Cobble/sand/clay
5th order	1,282	481-4049** (1246)	Cobble/sand/clay
7th order	37,007	9260-109586** (28883)	Silty sand/clay
8th order	65,948	0-96277** (18066)	Silty sand/clay

Table 2. Surface water background concentrations from samples collected during Spring 2016. 7th_A and 7th_B represent sites upstream and downstream of the Albuquerque waste water treatment plant, respectively.

Site	NO_3-N (mg L^{-1})	PO_4 (mg L^{-1})
1st	0.063	n.a.
2nd	0.226	n.a.
3rd	0.002	n.a.
4th	0.047	0.105
5th	0.034	0.077
7th_A	0.074	n.a.
7th_B	0.524	1.619
8th	0.097	0.414

In October 2015, we started the *in-situ* incubation of six packed columns (two replicates per substrate) in each study site. The columns were anchored to the streambed using H-shaped fence post body frame (See Figure S2), and were positioned parallel to the flow above the streambed to promote the colonization of the native biological communities

within the sediments. All columns were incubated for ~3 months. Following the *in-situ* incubation, the columns were retrieved between February and March 2016, except for the 3rd order stream, which was retrieved in early June 2016 due to high flows during the snowmelt season. After the columns were retrieved from the streams they were placed in a storage bin with unfiltered river water and brought to the Environmental Engineering laboratories at the University of New Mexico. In the laboratory, we filtered (0.7 µm GF/F filter; Sigma-Aldrich) stream water and connected the columns to a common (six heads) Masterflex peristaltic pump and perfused with filtered stream water until the beginning of the tracer experiments, which took place the day after column retrieval. Photographs of the mesocosms deployment and laboratory set up are provided in supporting information (Figure S1 and Figure S2).

Laboratory Tracer Experiments

For each study site, we conducted two types of resource supply injections: 1) only nitrate additions (nitrate experiments), and 2) stoichiometrically 'balanced' 106C:16N:1P additions (Redfield experiments). Each of these experiments was performed using one of the two columns with the same sediment texture (recall we have 6 columns per site; 2 replicates of 3 different sediment textures) (Figure 2). Our experiments allowed us to: 1) characterize hyporheic nitrate uptake in isolation of local hydrologic regimes (we used the same flow rate for all experiments), and 2) determine how nutrient resource supply influence nitrate uptake. In doing this, the variability unexplained by our experimental set up would be primarily due to differences in microbial function and abundance along the river continuum. Below, we explain the tracer experiments in detail.

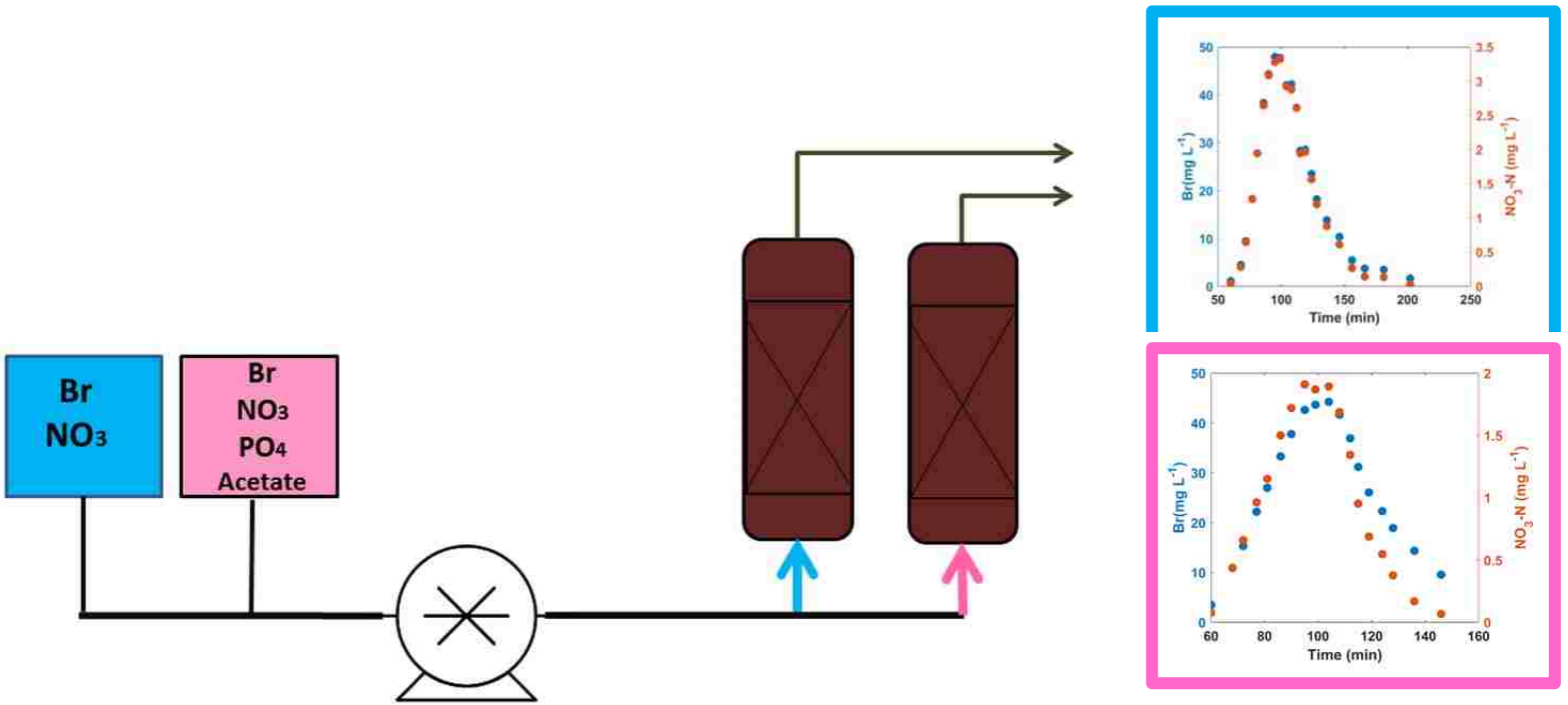

Figure 2. Mesocosm setup for one pair of replicate sediment textures for one study site along the Jemez-Rio Grande continuum. Colors indicate the different experiments performed (blue) only nitrate and conservative tracer and (pink) bromide and 106:16:1 C:N:P additions. Concentrations of bromide and nitrate were tracked over time at the end of the column, the breakthrough curves display experimental data found for native 7th_A.

Nitrate and conservative tracer additions- Nitrate experiments: After flushing the columns with filtered river water in the laboratory, we added a short-term pulse of filtered river water with sodium nitrate ($NaNO_3$) and the conservative tracer sodium bromide (NaBr) to one of the two replicate columns of each substrate from every site. The pulse was pumped against gravity at a constant rate of ~6 mL/min for ~40 min, which was the estimated time required to achieve 90% of the maximum, steady-state concentration at 20% of the total column length (L=0.1 m). After the pulse addition, we flushed the column with filtered river water for ~3 hours, at the same flow rate. We collected 20 mL aliquots over the duration of the experiment (injection and flushing) at the sampling port (L=0.5 m; at the end of the column), generating typical non-plateau tracer breakthrough curves. Samples were filtered immediately after collection using 0.45 µm Teflon membrane filters (DigiFILTER) and frozen at -20 ˚C until the day of analysis. Nitrate and bromide were analyzed within 1 month of sample collection using a Dionex ICS-1100 Ion Chromatograph (IC) with AS22/AG22 analytical and guard columns, and 100-µl injection loop. The analytical detection limits were 0.055 mg/L for NO_3 –N and 0.25 mg/L for bromide.

C, N and P and conservative tracer additions- Redfield experiments: In the second (same texture) column replicates from each site, we injected labile carbon (potassium acetate, CH_3CO_2K), $NaNO_3$ and sodium phosphate monohydrate ($NaH_2PO_4\_H_2O$) using an 'ideal', stoichiometrically balanced C:N:P addition following Redfield's ratio (i.e., 106 C: 16N: 1P), as well as NaBr. The injection, sampling technique, storage and analyses were performed under the same protocol described for the "nitrate experiments". Note that although we added C and P (we know the injectate concentrations), we did not track

the evolution of their concentrations in the sampling port, i.e., we only analyzed the samples for nitrate and bromide.

The injectate compositions (Table 3) were designed to simulate nitrate concentrations in impaired streams across the USA (USGS WaterQualityWatch). Furthermore, we doubled the concentrations of all the reagents in the 5th order stream to study biological nitrate under nutrient inputs that mimic concentrations of highly eutrophic streams.

Table 3. Injection solutions and targeted concentrations for a) 1st-4th and 7th-8th stream orders, and b) 5th stream order.

Tracer	**Injectate concentration "Nitrate Experiments" (mg L^{-1})**		**Injectate concentration "Redfield Experiments" (mg L^{-1})**	
	a)	b)	a)	b)
Nitrate (NO_3-N)	6	12	6	12
Bromide (Br)	65	131	65	131
Phosphate (PO_4)	n.a.	n.a.	2.5	5
Acetate (AcO^-)	n.a.	n.a.	547	1094

TASCC Analyses: Nutrient Spiraling Metrics

Dynamic Spiraling Metrics

We used the Tracer Addition for Spiraling Curve Characterization (TASCC) (Covino et al. 2010) method to estimate nitrate uptake dynamics. We calculated dynamic uptake lengths, $S_{w-add}\,(L)$, from each pair of co-sampled conservative (i.e. bromide) and reactive (i.e. nitrate) concentrations across the breakthrough curves observed in each column experiment:

$$S_{w-add} = -\frac{L}{\left[ln\left[\frac{NO_3 - N_{obs}}{Br_{obs}}\right] - ln\left[\frac{NO_3 - N_{IN}}{Br_{IN}}\right]\right]} \quad (1)$$

where $L\,(L)$ represents the length of the column and sampling distance; $NO_3 - N_{obs}(ML^{-3})$ is the background corrected concentration of nitrate observed in each grab sample; $Br_{obs}\,(ML^{-3})$ is the background corrected concentration of bromide observed in each grab sample; $NO_3 - N_{IN}\,(ML^{-3})$ is the concentration of nitrate in the injection, and $Br_{IN}\,(ML^{-3})$ is the concentration of bromide in the injection. Note that, as explained in Covino et al. (2010), uptake lengths in TASCC represent the same metrics that would result from conducting equal number of plateau enrichments with different steady-state concentrations, as was typically done before the TASCC method was developed (e.g., Mulholland et al., 2002; Dodds et al., 2002;Ensign and Doyle, 2006; Hall et al., 2013).

Using S_{w-add}, we calculated both dynamic areal uptake $U_{add}\,(M\,L^{-2}\,T^{-1})$ and dynamic uptake velocity $V_{f-add}\,(L\,T^{-1})$ for nitrate as:

$$U_{add} = \frac{Q * [NO_3 - N_{add}]}{S_{w-add} * w} \tag{2}$$

$$V_{f-add} = \frac{U_{add}}{[NO_3 - N_{add}]} \tag{3}$$

where $Q\,(L^3T)$, is experimental flow rate; $w\;\;(L)$ is the wetted column circumference $(2 * \pi * radius)$, and $NO_3 - N_{add}\,(M\,L^{-3})$ is the geometric mean concentration of the observed and conservatively transported nitrate concentration of the reactive tracer for each grab sample:

$$[NO_3 - N_{add}] = \sqrt{[NO_3 - N_{obs}] * [NO_3 - N_{cons}]} \tag{4}$$

where $NO_3 - N_{cons}\,(M\,L^{-3})$ is the background corrected concentration of the reactive tracer if it was conservatively transported.

To make comparisons across the different tracer tests conducted, we focused on the dynamic uptake velocity of the added nutrient, i.e., V_{f-add}. This variable represents the mass transfer coefficient and the demand for nutrients relative to their concentration (Webster and Valett, 2006). It is widely used to determine nutrient uptake efficiency across streams because it normalizes the uptake length by discharge (Davis and Minshall 1999), and areal uptake by concentration (Earl et al. 2006).

Ambient Spiraling Metrics

Following the TASCC method, we estimated nitrate ambient uptake lengths back extrapolating the intercept of the correlation between S_{w-add} and nitrate concentrations without background corrections, i.e., $NO_3 - N_{total}$ $(M\ L^{-3})$ (Covino et al., 2010). In the few instances for which back extrapolation provided negative intercept values, we calculated S_{w-amb} assuming the total nitrogen concentration was equal to the ambient nitrate concentration as suggested by Gibson et al. (2015). Once nitrate ambient uptake lengths were estimated, ambient areal uptake U_{amb} and ambient uptake velocity V_{f-amb} were determined by replacing $NO_3 - N_{add}$ with ambient nitrate concentration $NO_3 - N_{amb}$ in equations (2) and (3).

We determined total dynamic areal uptake for nitrate U_{tot} as the sum of ambient areal uptake U_{amb} and the dynamic areal uptake U_{add}. Total dynamic uptake velocity V_{f-tot} was calculated as:

$$V_{f-tot} = \frac{U_{tot}}{[NO_3 - N_{total}]} \quad (6)$$

Reactive tracer uptake kinetics

We used total (ambient + added) spiraling metrics to fit our data to the Michaelis-Menten (MM) model. We used uptake velocity rather than areal uptake because the latter uses

concentration as a factor and thus U_{tot} vs $NO_3 - N_{total}$ would result in a spurious correlation (Gonzalez-Pinzon et al., 2015; Day and Hall, 2017). The MM model was expressed in terms of V_{f-tot} is (Earl et al., 2006; O'Brien et al., 2007; Covino et al., 2010; Day and Hall, 2017):

$$V_{f-tot} = \frac{U_{max}}{K_s + [NO_3 - N_{total}]} \quad (7)$$

where U_{max} $(M\ L^{-2}\ T^{-1})$ corresponds to the maximum uptake at saturation and K_s $(M\ L^{-3})$ the half saturation constant.

Data synthesis

Statistical Synthesis

We incorporated repeated measurements of the injection solution as an indication of the uncertainty in the concentrations. For each experiment, we calculated the coefficient of variation (CV) of the replicates and used it to determine the upper and lower boundaries of the uncertainty in the measurements (i.e., $mean \pm (1 + CV)$. This uncertainty was considered during TASCC analysis when comparing $[NO_3 - N_{obs}: Br_{obs}]$ to $[NO_3 - N_{inj}: Br_{inj}]$.

We plotted the background-corrected ratio of the reactive to the conservative tracer concentrations for each grab sample $(\mathrm{NO_3 - N: Br})$ along with the same ratio for the concentrations of the injectate $(\mathrm{NO_3 - N_{Inj}: Br_{Inj}})$. Values of $(\mathrm{NO_3 - N: Br}) < (\mathrm{NO_3 - N_{Inj}: Br_{Inj}})$ indicate nitrate uptake, while higher ratios suggest a combination of non-reactive transport, potential minor systematic errors in measurements of concentrations close to the detection limit (error in signal being amplified mainly in the ratio at the beginning of the rising limb and end of the falling limb), or nitrate production.

We assumed that nitrate production is negligible because background samples collected at different time intervals before the experiment showed insignificant variations in nitrate concentration. Moreover, we did not add ammonium to the injection solution, thus potential nitrification can be disregarded, thus we excluded points above the injectate ($NO_3 - N_{Inj}: Br_{Inj}$) line. Furthermore, we identified and excluded outliers from our uptake kinetics relationships following the interquartile range criteria (Ensign and Doyle et al., 2006). We performed outlier selection for uptake lengths only, because uptake velocity and areal uptake depend on this metric. We excluded from the analysis S_{w-add} metrics outside the interquartile range, as well as, the V_{f-add} and U_{add} values associated with them.

We used linear regressions to determine the significance of the correlation between nutrient uptake lengths and total nutrient concentrations. Differences in uptake metrics for NO_3-N across stream orders and different substrates were examined using the Kruskal-Wallis test (KW), which is a non-parametric analysis of variance for data that are not normally distributed (Ensign and Doyle et al., 2006). We used an alpha value of 0.05 for significance in all statistical tests.

The differences between uptake velocities in the nitrate experiments vs the Redfield experiments were examined for each stream order and substrate using a Mann-Whitney U test (Ensign and Doyle, 2006), which is a non-parametric statistical test for data that are not normally distributed and have large differences in sample size among groups.

We evaluated the fitting of the maximum uptake fluxes U_{max} and half-saturation constants K_s in the MM model using non-linear least squares regression (Wollheim et al., 2006). We conducted all statistical analyses using MATLAB (R2016b).

Model Synthesis

We fitted a MM model to V_{f-tot} vs $NO_3 - N_{total}$ to evaluate the hyporheic nutrient processing kinetics. We studied only saturation kinetics because at different magnitudes of nutrient concentration, the MM equation is capable of describing other kinetic models (Bekins et al., 1998).

At low concentrations ($NO_3 - N_{total} \ll K_s$), areal uptake approximates a linear relationship with increasing nutrient concentration and uptake length and velocity remain constant with nutrient concentration, evidencing 1st-order nutrient kinetics (O'Brien et al., 2007). As nutrient concentration increases, areal uptake increases to an asymptotic plateau and uptake velocity decreases exponentially with nutrient concentration, indicating the system is approaching saturation (cf. efficiency loss (EL) model in O'Brien et al., 2007). This behavior is maintained until uptake remains constant with increasing concentration and thus the system is considered to be saturated (Earl et al., 2006).

When fitting our data to MM equation, the system was considered to be saturated if there was a significant fit (R^2 and p-value) of model parameters and if the numeric value found for K_s was within the experimental concentrations (O'Brien et al., 2007). If these conditions were not met, the system did not reach saturation and could be better represented by 1st order kinetics or EL. Since saturation at higher nutrient concentrations is expected (Dodds et al., 2002), K_s and U_{max} of non-saturated systems were calculated for reference.

RESULTS

Ambient Metrics

Ambient NO_3-N concentrations were low and varied from the detection limit 0.055 to 0.344 mg L^{-1} NO_3-N (**Table 4**). Ambient metrics varied across sites, sediments and tracer experiments (Table 5 Table 6). For the nitrate experiments, ambient uptake lengths (S_{w-amb}) ranged from 0.1-13 m (CV = 1.1). Ambient uptake velocities (V_{f-amb}) ranged from 0.002-0.14 mm min^{-1} (CV = 1.27), and ambient areal uptakes (U_{amb}) ranged from 0.13 to 30.4 µg m^{-2} min^{-1}(CV = 2.17). For Redfield experiments, S_{w-amb} ranged from 0.1-7.1 m (CV = 1.02), V_{f-amb} ranged from 0.004-0.721 mm min^{-1} (CV = 1.99), and U_{amb} varied across experiments from 0. 3 to 116.7 µg m^{-2} min^{-1}(CV = 2.64).

Table 4. Ambient NO_3-N concentrations in mg L^{-1} NO_3-N from samples collected 1 hour prior the injection (after overnight column flushing with water from respective sites). Values below the detection limit of the instrument were fixed to 0.055 mg L^{-1} NO_3-N.

Stream Order	Native		Gravel		Silica sand	
	Nitrate	Redfield	Nitrate	Redfield	Nitrate	Redfield
1st	0.170	0.320	0.305	0.055	0.055	0.055
2nd	0.055	0.055	0.135	0.111	0.227	0.055
3rd	0.187	0.162	0.055	0.055	0.055	0.055
4th	0.055	0.115	0.055	0.055	0.055	0.151
5th	0.102	0.094	0.055	0.055	0.055	0.055
7th_A	0.055	0.055	0.055	0.055	0.055	0.055
7th_B	0.339	0.066	0.055	0.055	0.055	0.055
8th	0.055	0.344	0.055	0.055	0.055	0.055

Table 5. Ambient spiraling metrics calculated from back extrapolated ambient uptake lengths for nitrate experiments.

	Native			Gravel			Silica sand		
	Sw_{amb} (m)	**Vf_{amb} (mm min^{-1})**	**U_{amb}(µg m^{-2} min^{-1})**	**Sw_{amb} (m)**	**Vf_{amb} (mm min^{-1})**	**U_{amb}(µg m^{-2} min^{-1})**	**Sw_{amb} (m)**	**Vf_{amb} (mm min^{-1})**	**U_{amb}(µg m^{-2} min^{-1})**
1^{st}	1.0	0.031	5.2	4.4	0.007	2.2	12.4	0.003	0.1
2^{nd}	2.2	0.015	0.7	2.0	0.016	2.1	13.0	0.002	0.6
3^{rd}	0.9	0.037	7.0	1.5	0.022	1.1	1.4	0.023	1.2
4^{th}	1.3	0.024	1.2	1.8	0.018	0.9	2.6	0.012	0.6
5^{th}	1.6	0.020	2.0	2.1	0.015	0.8	1.4	0.022	1.1
7^{th} $\bar{A}$	1.0	0.032	1.6	2.0	0.016	0.8	3.1	0.010	0.5
7^{th} $\bar{B}$	0.4	0.090	30.4	11.8	0.003	0.1	8.5	0.004	0.2
8^{th}	0.2	0.142	7.1	2.3	0.014	0.7	5.9	0.005	0.3

Table 6. Ambient spiraling metrics calculated from back extrapolated ambient uptake lengths for Redfield experiments.* Uptake lengths calculated following Gibson et al. (2015).

	Native			Gravel			Silica sand		
	Sw_{amb} (m)	**Vf_{amb} (mm min^{-1})**	**U_{amb}(µg m^{-2} min^{-1})**	**Sw_{amb} (m)**	**Vf_{amb} (mm min^{-1})**	**U_{amb}(µg m^{-2} min^{-1})**	**Sw_{amb} (m)**	**Vf_{amb} (mm min^{-1})**	**U_{amb}(µg m^{-2} min^{-1})**
1^{st}	1.1	0.030	9.6	1.4	0.022	1.1	3.3	0.010	0.5
2^{nd}	1.1	0.030	1.5	3.8	0.008	0.9	5.3	0.006	0.3
3^{rd}	0.1*	0.721	116.7	0.4	0.078	3.9	1.1	0.029	1.4
4^{th}	7.1	0.004	0.5	1.2	0.026	1.3	1.9	0.017	2.5
5^{th}	1.3	0.025	2.3	1.5	0.021	1.0	1.7	0.019	0.9
7^{th} $\bar{A}$	0.3	0.105	5.2	0.9	0.036	1.8	2.4	0.013	0.7
7^{th} $\bar{B}$	0.3	0.099	6.6	0.5	0.058	2.9	5.1	0.006	0.3
8^{th}	0.3	0.122	41.5	0.1*	0.281	14.0	4.1	0.008	0.4

NO_3-N uptake

For simplicity, in this section we describe the numerical results from each experiment performed as the combination of metrics found for all the stream orders with the same substrate. Tables S1 and Table S2 in the supporting information provide detailed results for nitrate and Redfield experiments respectively, as well as, a summary from the results associated to each stream order, with a combination of different sediment textures (last column), and a summary of the results obtained for all stream orders as function of substrate (last row).

Nitrate experiment

For native sediments, and all stream orders, S_{w-add} averaged 1.82 m (median 1.91 m) and ranged from 0.1 to 4.4 m (CV =0.48). The average V_{f-add} was 0.03 mm min^{-1} (median 0.02 mm min^{-1}), and ranged from 0.007 to 0.224 mm min^{-1} (CV=1.15), and U_{add} averaged 25.05 µg m^{-2} (median 21.85 µg m^{-2}), and ranged from 0.6 to 83.3 µg m^{-2} min^{-1} (CV=0.68). For gravel, S_{w-add} averaged 3.58 m (median 2.35 m) and ranged from 0.4 to 14.1 m (CV =0.74). The average V_{f-add} was 0.01 mm min^{-1} (median 0.01 mm min^{-1}), and ranged from 0.002 to 0.071 mm min^{-1} (CV=0.68), and U_{add} averaged 16.97 µg m^{-2} (median 11.64 µg m^{-2}) and ranged from 0.6 to 75.8 µg m^{-2} min^{-1} (CV=0.82). For silica sand, uptake length averaged 5.88 m (median 3.20 m) and ranged from 1.0 to 54.6 m (CV =1.33). The average V_{f-add} was 0.01 mm min^{-1} (median 0.01 mm min^{-1}), and ranged from 0.001 to 0.032 mm min^{-1} (CV=0.63), and U_{add} averaged 28.54 µg m^{-2} (median 17.34 µg m^{-2}) and ranged from 0.04 to 227.8 µg m^{-2} min^{-1} (CV=1.30).

Redfield experiment

For native sediments, and all stream orders, S_{w-add} averaged 1.82 m (median 1.37 m) and ranged from 0.1 to 14.2 m (CV =1.10). The average V_{f-add} was 0.04 mm min^{-1} (median 0.02 mm min^{-1}) and ranged from 0.002 to 0.406 mm min^{-1} (CV=1.22), and U_{add} averaged 32.78 µg m^{-2} (median 22.77 µg m^{-2}), and ranged from 0.3 to 127.1 µg m^{-2} min^{-1} (CV=0.93). For gravel, S_{w-add} averaged 1.78 m (median 1.50 m) and ranged from 0.2 to 6.2 m (CV =0.90). The average V_{f-add} was 0.03 mm min^{-1} (median 0.02 mm min^{-1}), and ranged of 0.005 to 0.195 mm min^{-1} (CV=0.95), and U_{add} averaged 18.24 µg m^{-2} (median 14.07 µg m^{-2}), and ranged from 1.1 to 69.9 µg m^{-2} min^{-1} (CV=0.79). For silica sand, S_{w-add} averaged 3.52 m (median 3.22 m) and ranged from 0.3 to 12.0 m (CV =0.64). The average V_{f-add} was 0.02 mm min^{-1} (median 0.01 mm min^{-1}), and ranged from 0.003 to 0.121 mm min^{-1} (CV=1.33) and U_{add} averaged 31.50 µg m^{-2} (median 19.53 µg m^{-2}) and ranged from 0.2 to 256.6 µg m^{-2} min^{-1} (CV=1.30).

Overall patterns of nutrient uptake metrics

For most experiments, S_{w-add} increased with nutrient concentrations, V_{f-add} was negatively correlated with $NO_3 - N_{total}$ (Figure 3) and U_{add} was positively correlated with $NO_3 - N_{total}$, following both linear and exponential trends (Figure 4). However, we encountered some cases where S_{w-add} decreased with increase in $NO_3 - N_{total}$ and V_{f-add} was positively correlated with $NO_3 - N_{total}$ (Figure 3.e 1st and 2nd order). We also found some scenarios where no relationship could be found between these two metrics (S_{w-add} and V_{f-add}) and concentration but strong positive linear relationship was present between U_{add} and $NO_3 - N_{total}$ because this plot generates a spurious

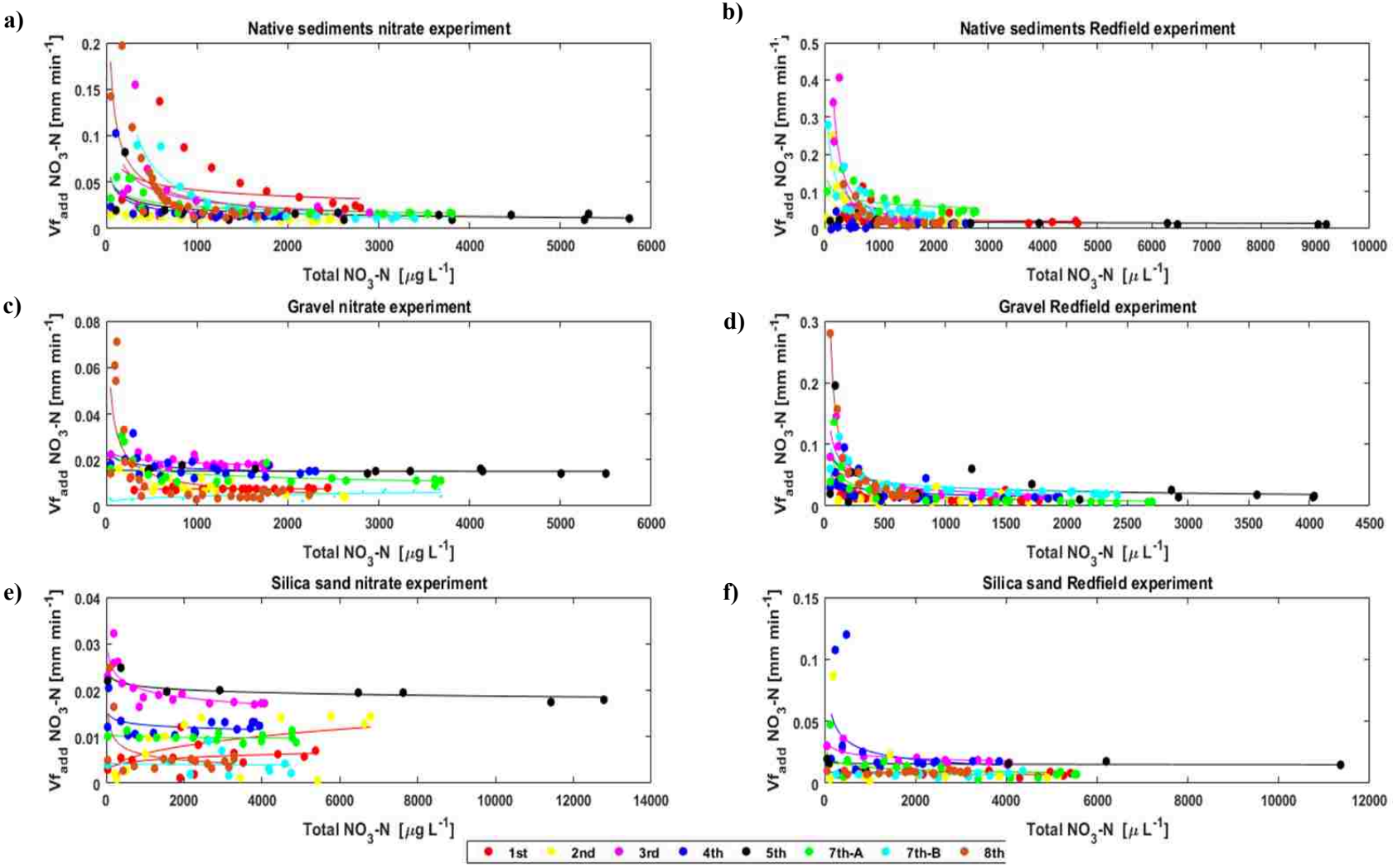

Figure 3. (a-f) Nitrate uptake velocities ($\boldsymbol{V_{f-add}}$ NO_3-N) as a function of total nitrate concentration for the both tracer additions (nitrate and Redfield) and sediment textures. Symbols represent experimental data from grab samples, solid lines follow a power function for reference, and different colors indicate stream orders as denoted in the legend.

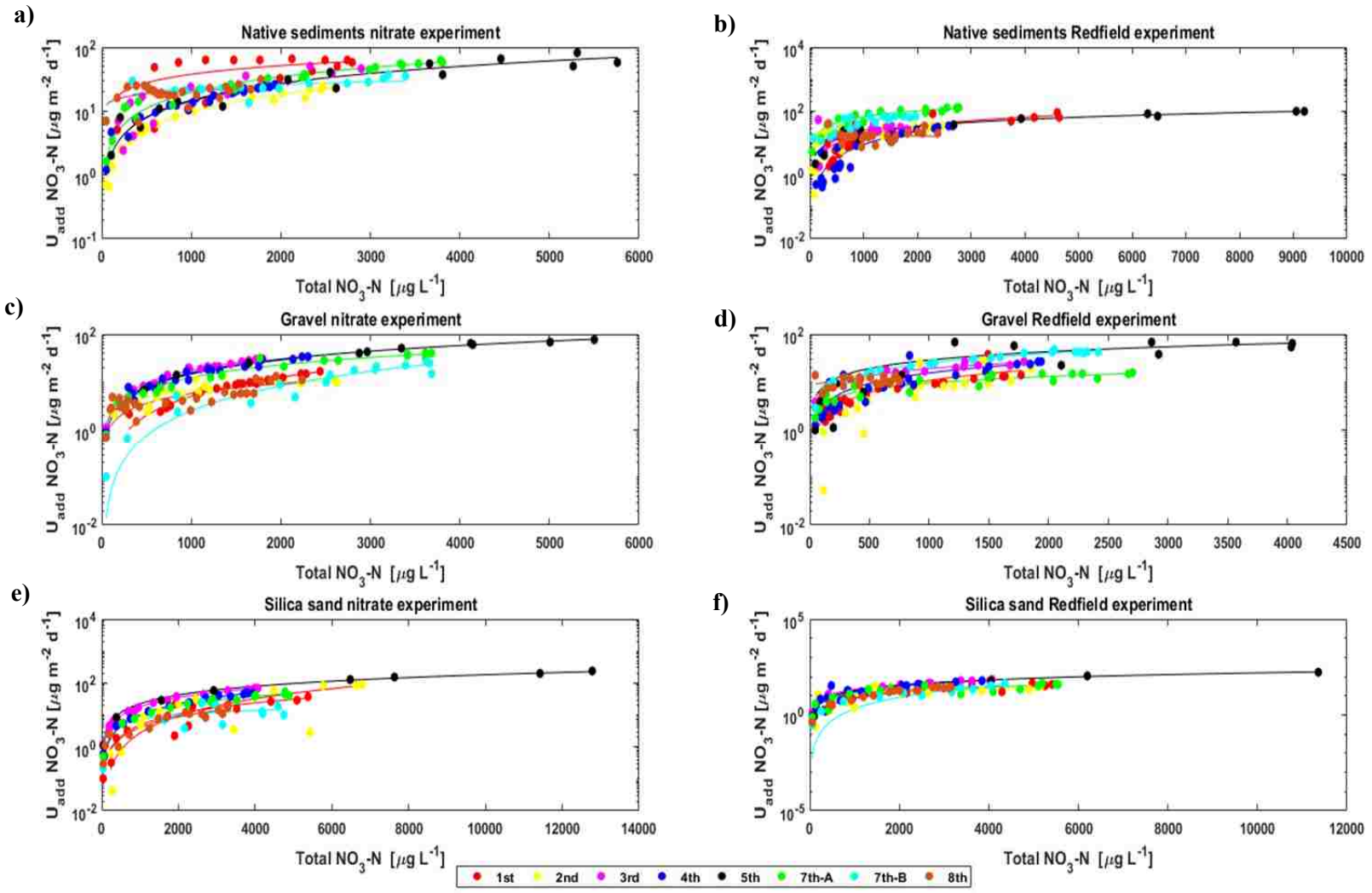

Figure 4. (a-f) Nitrate areal uptake rate ($\boldsymbol{U_{add}}$ NO_3-N) as a function of total nitrate concentration for the both tracer additions (nitrate and Redfield) and sediment textures. Symbols represent experimental data from grab samples, solid lines follow a power function for reference, and different colors indicate stream orders as denoted in the legend.

correlation (not mechanistically, i.e., based on MM model, but numerically, i.e., based on how we actually compute U from concentration data, using the nutrient spiraling metrics developed in the literature).

The slopes of the regressions associated with uptake length for native sediments across stream orders and tracer experiments showed different patterns in the rising and falling limb suggesting hysteresis behaviors (i.e., positive or negative relationships). The hysteresis present in S_{w-add} was consistently carried through the calculation of V_{f-add} and U_{add} (Figures 5 and 6). Numerically, these spiraling parameters were different for comparable NO_3-N concentrations, suggesting stronger uptake in the falling limb.

Although different studies have reported the presence of hysteresis in uptake length metrics during TASCC additions in stream ecosystems (Trentman et al. 2014, Gibson et al. 2015, Rodriguez-Cardona et al. 2016; Day and Hall, 2017), the interpretation of the behavior has received little attention. Covino et al. (2010) addressed potential hysteresis effects for estimating spiraling metrics. They proposed a variable travel time approach to identify and quantify temporal dependencies in V_{f-add} and U_{add} spiraling parameters, however since we observed hysteresis also in S_{w-add}, the variable travel time approach could not contribute to new interpretation of the patterns observed.

Currently, two methods have been used to consider hysteresis in nutrient uptake metrics analyses: (1) use the whole breakthrough curve regardless of the patterns (Covino et al. 2010, Gibson et al. 2015, Trentman et al. 2015), and (2) work with only the falling limb (Day and Hall, 2017). We tested the effect of the hysteresis in the extrapolation of S_{w-amb} by comparing the value extrapolated for the entire curve with that resulting from the falling limb. For some experiments, we found negative ambient uptake lengths when

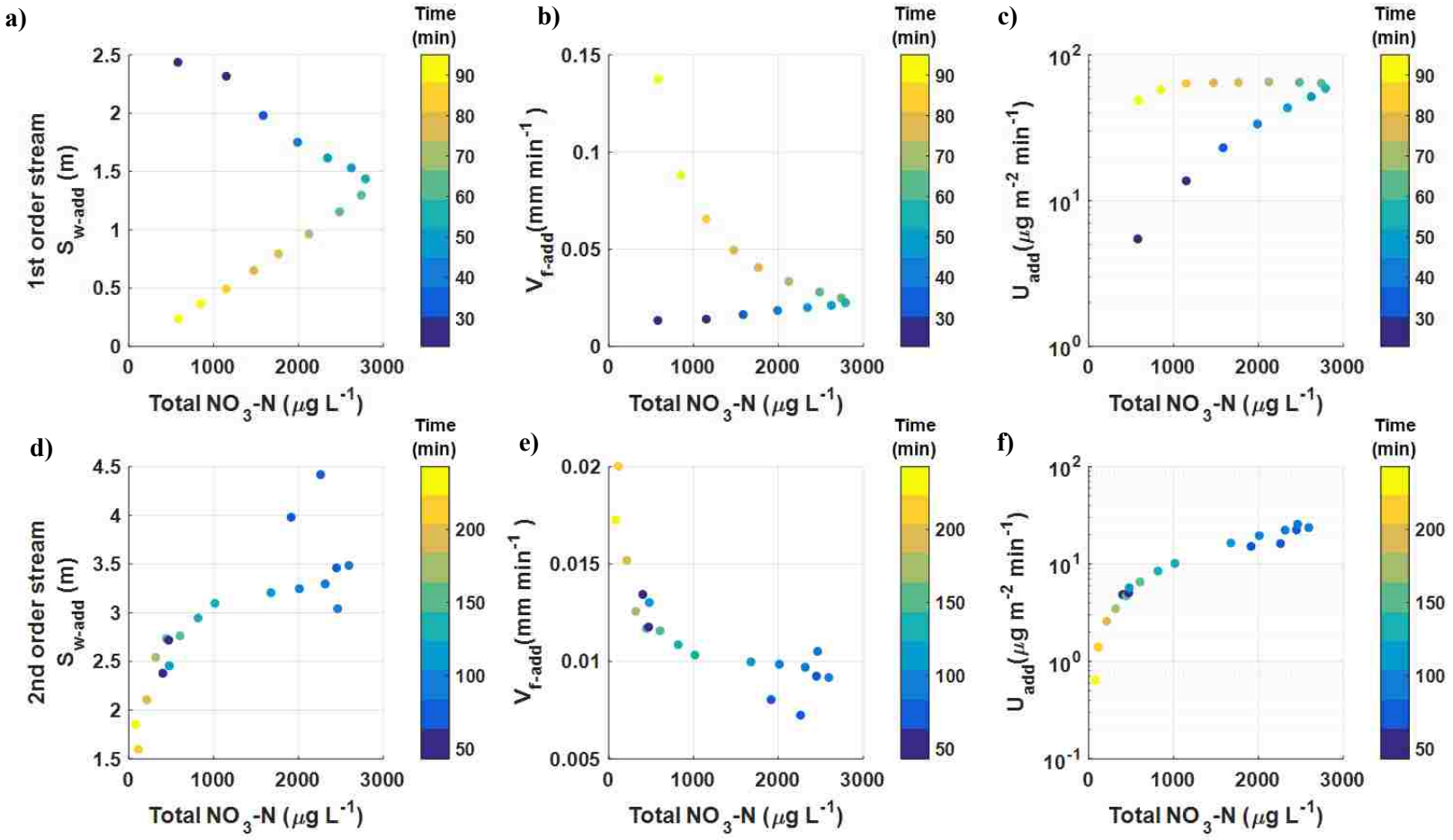

Figure 5. (a-f) Uptake length ($\boldsymbol{S_{w-add}}$), uptake velocity ($\boldsymbol{V_{f-add}}$) and areal uptake rate ($\boldsymbol{U_{add}}$) as a function of total nitrate concentration during nitrate experiments. (a-c) show results from 1st order native sediments columns and (d-f) show results from 2nd order native sediments columns. Symbols correspond to grab samples; different colors are associated with the time the samples were collected. Clockwise hysteresis can be observed across metrics.

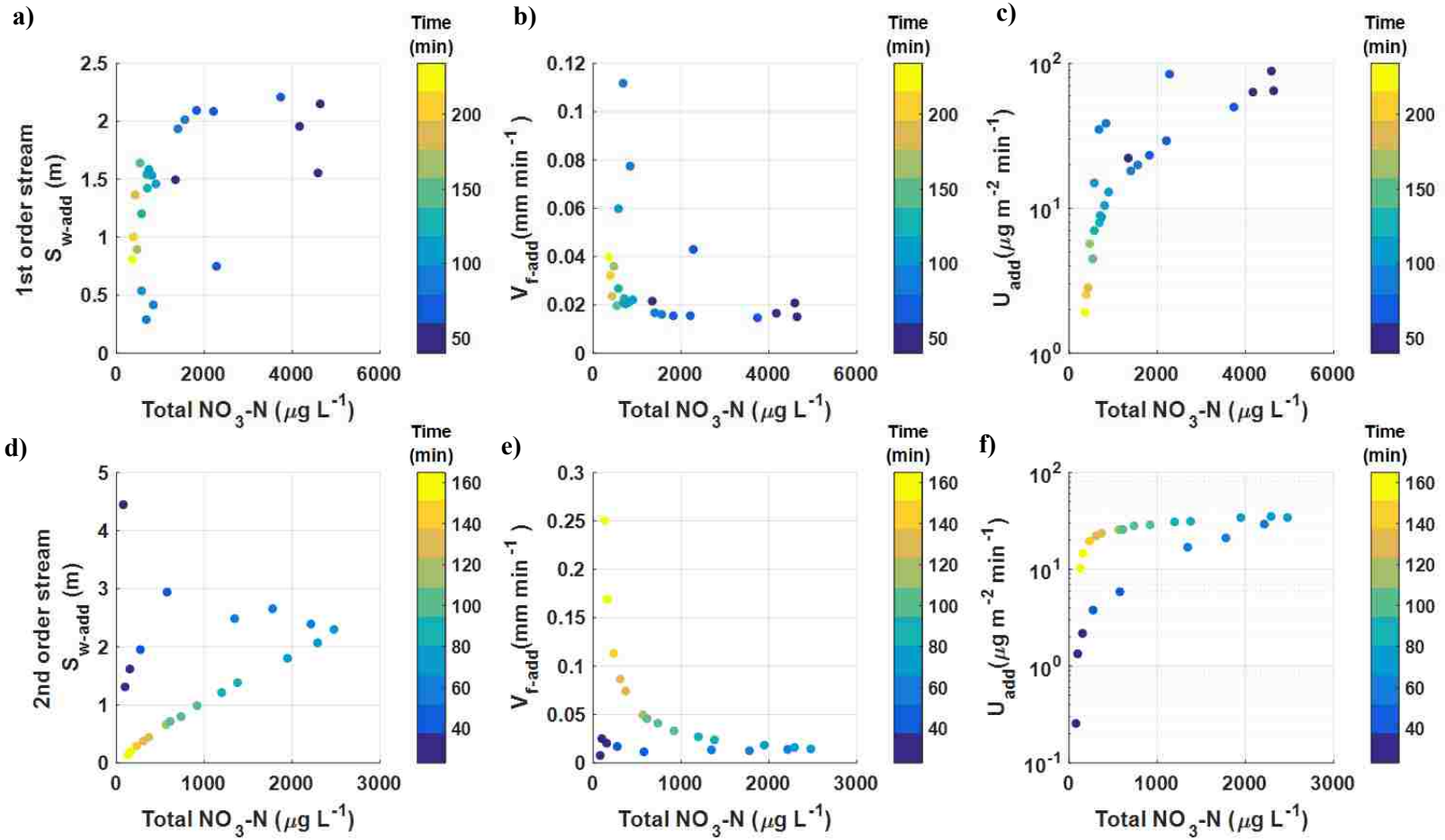

Figure 6. (a-f) Uptake length ($\boldsymbol{S_{w-add}}$), uptake velocity ($\boldsymbol{V_{f-add}}$) and areal uptake rate ($\boldsymbol{U_{add}}$) as a function of total nitrate concentration during Redfield experiments. (a-c) show results from 1st order native sediments columns and (d-f) show results from 2nd order native sediments columns. Symbols correspond to grab samples; different colors are associated with the time the samples were collected. Clockwise hysteresis can be observed across metrics.

considering just the falling limb (even after applying the correction suggested by Gibson et al., 2015), and for others we found ambient uptake lengths with standard deviations ranging from 0.05-0.7(except for the 4th order, Redfield experiment with native sediments, where we found a standard deviation of 3.80). Since the results varied from uptake lengths without physical meaning to values within the same order of magnitudes, the dynamic spiraling metrics discussed in this study represent a combination of all the values in the breakthrough curve to better represent the processes that could be affecting uptake within the columns (i.e. more conservative transport of NO_3-N in the rising limb and stronger uptake in the falling limb).

NO_3-N Kinetic Models

NO_3-N kinetic parameters

For simplicity, in this section we describe the numerical results from experiments whose fitted kinetic metrics showed saturated or close to saturation conditions. We present these metrics as a combination of the parameters found for all the stream orders with the same substrate. Table 7 and Table 8 provide detailed results for nitrate and Redfield experiments, each stream order, different sediment textures, as well as kinetically saturated and non-saturated columns.

Nitrate experiment

For native sediments K_s averaged 1547 µg L-1 (median 1399 µg L-1) and ranged from 192 to 3082 µg L-1. U_{max} averaged 66 µg m-2 min-1 (median 66 µg m-2 min-1) and ranged from 30 to 136 µg m-2 min-1. For gravel experiments K_s averaged 3168 µg L-1 (median 3568 µg L-1) and ranged from 198 to 5981 µg L-1. U_{max} averaged 65 µg m-2 min-1 (median 68 µg m-2 min-1) and ranged from 8 to 132 µg m-2 min-1. For silica sand

Table 7. NO_3-N uptake parameters for nitrate experiments derived from Michaelis-Menten model at each stream order and sediment texture.

	Native				Gravel				Silica sand			
Stream order	**MM Umax (µg m^{-2} min^{-1})**	**MM Ks (µg L^{-1})**	**MM R^2**	**Saturation (Y/N)**	**MM Umax (µg m^{-2} min^{-1})**	**MM Ks (µg L^{-1})**	**MM R^2**	**Saturation (Y/N)**	**MM Umax (µg m^{-2} min^{-1})**	**MM Ks (µg L^{-1})**	**MM R^2**	**Saturation (Y/N)**
1st	136	2371	0.18	Y	6.51E+05	8.91E+07	-0.06	N	4.81E+06	9.24E+08	-0.08	N
2nd	47	3082	0.79	N	19	1082	0.71	Y	4.28E+07	5.48E+09	-0.08	N
3rd	67	1307	0.51	Y	132	5981	0.50	N	179	7407	0.58	N
4th	30	805	0.50	Y	99	5012	0.24	N	1.65E+06	1.37E+08	-0.07	N
5th	78	2742	0.37	Y	1231	79141	0.08	N	1008	45255	0.72	N
7th_A	65	1491	0.71	Y	68	3568	0.41	Y	698	67953	0.07	N
7th_B	70	383	0.96	Y	4.74E+06	9.74E+08	-0.07	N	71	14573	0.03	N
8th	38	192	0.87	Y	8	198	0.65	Y	18	1895	0.29	Y

Table 8. NO_3-N uptake parameters for Redfield experiments derived from Michaelis-Menten model at each stream order and sediment texture.

	Native				Gravel				Silica sand			
Stream order	**MM Umax (µg m^{-2} min^{-1})**	**MM Ks (µg L^{-1})**	**MM R^2**	**Saturation (Y/N)**	**MM Umax (µg m^{-2} min^{-1})**	**MM Ks (µg L^{-1})**	**MM R^2**	**Saturation (Y/N)**	**MM Umax (µg m^{-2} min^{-1})**	**MM Ks (µg L^{-1})**	**MM R^2**	**Saturation (Y/N)**
1st	149	4098	0.20	N	20	692	0.53	Y	177	20610	0.12	N
2nd	65	1140	0.28	Y	127	10098	0.01	N	28	1413	0.13	Y
3rd	87	100	0.99	Y	30	281	0.96	Y	125	3995	0.81	Y
4th	6.59E+06	7.28E+08	-0.05	N	32	837	0.33	Y	82	2693	0.10	Y
5th	149	5255	0.48	Y	157	4663	0.15	N	4207	255400	0.008	N
7th_A	205	1742	0.62	Y	16	250	0.90	Y	53	2743	0.38	Y
7th_B	52	134	0.78	Y	50	636	0.89	Y	1193	162212	0.001	N
8th	69	198	0.96	Y	28	50	0.98	Y	1.21E+06	1.36E+08	-0.07	N

only the 8th order reached saturation with K_s 1895 µg L-1and U_{max} 18 µg m-2 min-1.

Redfield experiment

For native sediments K_s averaged 1810 µg L^{-1}(median 1140 µg L^{-1}) and ranged from 100 to 5255 µg L^{-1}. U_{max} averaged 111 µg m^{-2} min^{-1} (median 87 µg m^{-2} min^{-1}) and ranged from 52 to 205 µg m^{-2} min^{-1}. For gravel experiments K_s averaged 1058 µg L^{-1}(median 636 µg L^{-1}) and ranged from 50 to 4663 µg L^{-1}. U_{max} averaged 47 µg m^{-2} min^{-1} (median 30 µg m^{-2} min^{-1}) and ranged from 16 to 157 µg m^{-2} min^{-1}. For silica sand K_s averaged 2711 µg L^{-1}(median 2718 µg L^{-1}) and ranged from 1413 to 3995 µg L^{-1}. U_{max} averaged 72 µg m^{-2} min^{-1} (median 68 µg m^{-2} min^{-1}) and ranged from 28 to 125 µg m^{-2} min^{-1}.

Overall patterns of Kinetic Models

The kinetic response of V_{f-tot} varied across experimental additions and substrates. Saturation (and proximity to saturation, i.e., V_{f-tot} decrease with nutrient concentration) was predominant in native sediments and gravel, primarily observed during Redfield additions. Silica sand columns were considered far from saturation, since for most experiments V_{f-tot} appeared to be constant with respect to $NO_3 - N_{total}$. Moreover, silica sand metrics for 1st and 2nd order streams in the nitrate experiment had a positive correlation between V_{f-tot} and $NO_3 - N_{total}$.

NO_3-N Uptake in Nitrate vs Redfield experiments

The efficiency of nitrate processing under different stoichiometric limitations varied with stream order and substrate (Figure 7Figure 8). Median V_{f-add} were higher during Redfield injections for most of the experiments (16 out of 24 comparisons). However, the magnitudes of median U_{add} (not plotted) were similar across experiments and did not

increase or decrease across experiments with the same pattern observed for V_{f-add}. Table 9 and Table 10 present a summary of the variability between the median addition uptake velocity and areal uptake in each of the experiments performed.

Table 9. Comparison between median NO_3-N uptake velocity in nitrate and Redfield experiments by stream order and sediment texture. *p<0.05, ** p<0.001. Statistically significance based on Mann-Whitney U test.

	Native			**Gravel**			**Silica sand**		
	$Vf_{add\ MED}$ (mm min^{-1})			**$Vf_{add\ MED}$ (mm min^{-1})**			**$Vf_{add\ MED}$ (mm min^{-1})**		
Stream order	***Nitrate***	***Redfield***		***Nitrate***	***Redfield***		***Nitrate***	***Redfield***	
1st	0.025	0.021	↓	0.006	0.013	↑**	0.006	0.007	↑
2nd	0.011	0.024	↑**	0.007	0.011	↑	0.010	0.005	↓
3rd	0.024	0.030	↑	0.018	0.023	↑	0.018	0.019	↑
4th	0.014	0.011	↓**	0.015	0.015	←	0.012	0.017	↑*
5th	0.015	0.015	←	0.015	0.019	↑	0.019	0.016	↓*
7th_A	0.017	0.051	↑**	0.011	0.008	↓	0.010	0.009	↓
7th_B	0.017	0.050	↑**	0.005	0.024	↑**	0.003	0.007	↑*
8th	0.025	0.020	↓*	0.006	0.0325	↑**	0.005	0.009	↑**

Table 10. Comparison between median NO_3-N aerial uptake in nitrate and Redfield experiments by stream order and sediment texture. *p<0.05, ** p<0.001. Statistically significance based on Mann-Whitney U test.

	Native			**Gravel**			**Silica sand**		
	$U_{add\ MED}$ (µg m^{-2} min^{-1})			**$U_{add\ MED}$ (µg m^{-2} min^{-1})**			**$U_{add\ MED}$ (µg m^{-2} min^{-1})**		
Stream order	***Nitrate***	***Redfield***		***Nitrate***	***Redfield***		***Nitrate***	***Redfield***	
1st	57.2	16.4	↓*	9.26	6.38	↓	15.1	23.1	↑
2nd	8.37	22.6	↑*	6.20	7.62	↑	12.7	13.9	↑
3rd	19.0	25.2	↑	20.7	16.7	↓	24.6	45.8	↑
4th	17.3	7.3	↓	17.2	9.2	↓	24.9	22.7	↓
5th	34.7	46.9	↑**	41.6	38.9	↓	124.8	64.4	↓
7th_A	33.3	88.3	↑	17.6	10.6	↓	27.8	20.7	↓
7th_B	23.0	58.0	↑*	13.6	29.7	↑*	11.3	15.6	↑
8th	21.0	16.4	↓*	4.38	10.7	↑*	8.3	18.3	↑*

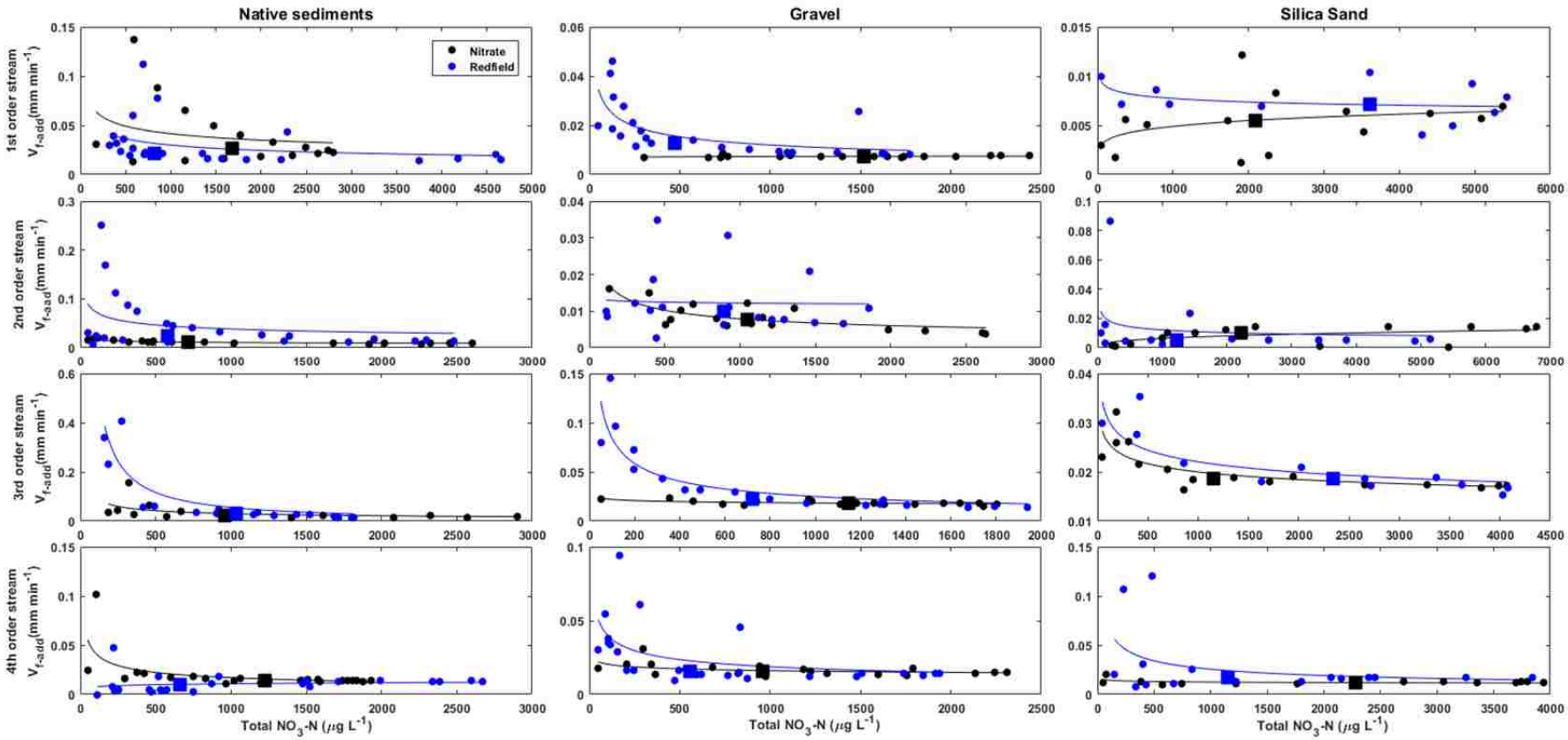

Figure 7. Comparison between nitrate and Redfield uptake velocities ($\boldsymbol{V_{f-add}}$) curves each sediment texture from 1st to 4th order streams. Nitrate additions are shown in black, and Redfield additions are shown in blue. Circles represent grab samples, squares represent the median uptake velocities per data set and solid lines show a power fit for reference.

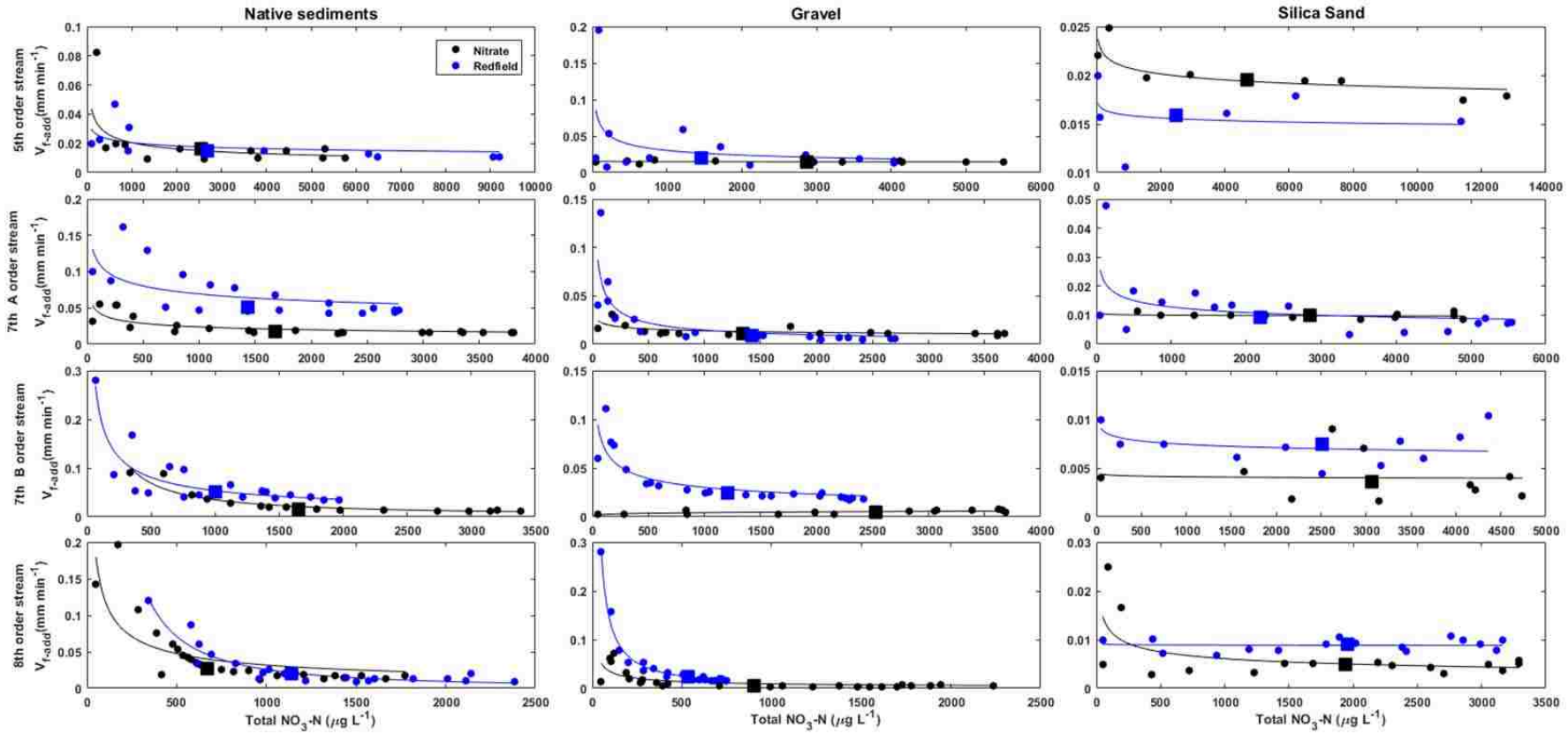

Figure 8. Comparison between nitrate and Redfield uptake velocities ($\boldsymbol{V_{f-add}}$) curves each sediment texture from 5th to 8th order streams. . Nitrate additions are shown in black, and Redfield additions are shown in blue. Circles represent grab, squares represent the median uptake velocity solid lines fit to a power function for reference.

DISCUSSION

We quantified NO_3-N uptake dynamics along a river continuum using column experiments. This allowed us to us to replicate vertical flow through the top 50 cm of the sediment-water interface, where most ecologically important biochemical reactions are known to occur (Navel et al., 2009; Harvey et al., 2013; Knapp et al., 2017).

NO_3-N uptake and spatial variability

Nitrate uptake velocities for native sediments were usually higher within the same type of experiment and different sediments (Figure 9), indicating more efficient nitrate removal. Highest V_{f-add} values were found in the Redfield experiments with native sediments and our estimates corresponded to the lower end of ranges reported in the literature for headwater streams (e.g., Ensign and Doyle, 2006; O'Brien et al., 2007; Mulholland et al., 2008; Tank et al., 2008; Wollheim et al., 2014).

The behavior of U_{add} and V_{f-add} with respect to $NO_3 - N_{total}$ followed the patterns observed in several studies (Stream Solute Workshop, 1990; Dodds et al., 2002; Mulholland et al., 2002; Earl et al., 2007; O 'Brien e t al., 2007; Hall et al., 2009; Covino et al., 2010; Ribot et al., 2013). The hysteresis found in the native sediments suggested that stronger uptake occurred in the falling limb of the breakthrough curve due to longer residence times. Weaker uptake in the rising limb may be associated to more conservative transport of the reactive tracer influenced by preferential flow paths created within the column.

Nitrate uptake spiraling metrics across substrates and stream orders were different (KW $p<0.0001$). Due to the differences in the injection concentration, spiraling metrics for the

5th order stream explored higher ranges of concentrations but overall the efficiency of the system to remove nitrate ($V_{f-median}$) was similar to the efficiency of streams with lower injection concentrations (Table S1 and Table S2), suggesting that microbes were not affected by the short-term, high nutrient input. Uptake velocities from the native sediments were generally higher. Although common substrates (silica sand and gravel) were used to standardize biological uptake removing the effects of site-dependent soil textures along the continuum, our results did not follow similar uptake patterns for a given standard sediment texture. This could be due to differences in the microbial colonization, which could be a function of the site-specific flow regimes and microbial abundances in the stream water during the incubation period. However, our experiments could not resolve this conundrum.

Hall et al., (2013) compiled in-stream nutrient uptake data from 969 separate nutrient uptake experiments and found that nitrate S_w generally decreased with stream order. Contrary to these findings, our results suggest that solute-specific nitrate uptake processes cannot be easily scaled along the river continuum. Moreover, our data show that median uptake velocities were comparable across columns for the same substrate and injections (CV range 0.11-0.55), but since uptake velocities were different across stream orders (KW $p<0.001$), there is not sufficient information available to validate the hypothesis proposed by Wollheim et al. (2006), which suggests that nutrient demand can be considered constant throughout the river network.

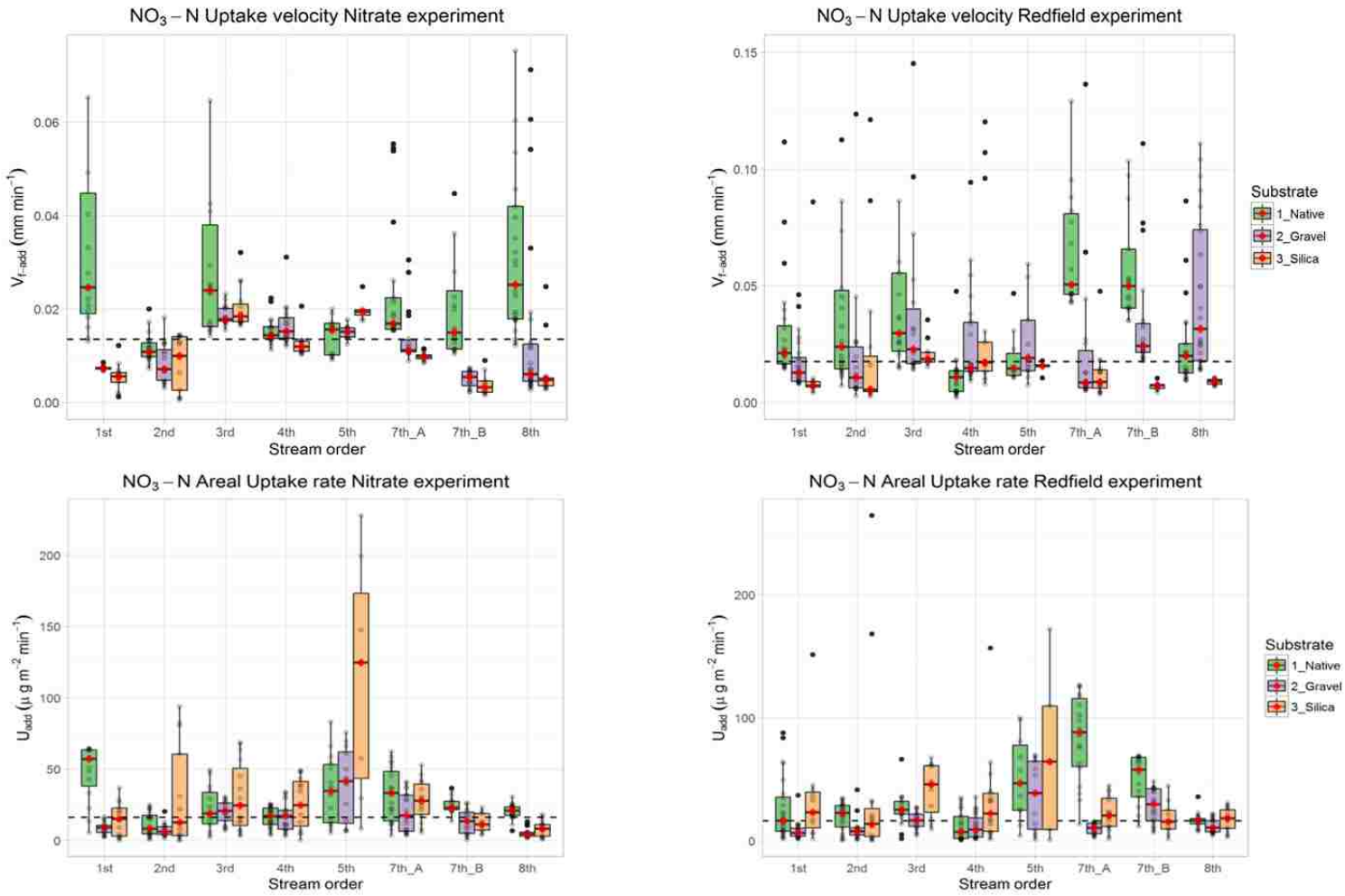

Figure 9. (a-b) Uptake velocities and (c-d) areal uptake rates for nitrate and Redfield additions in mesocosms along the Jemez River-Rio Grande continuum. Color represent sediment textures, the dotted line represents the global data median and the red diamonds individual median of the dataset.

NO_3-N Uptake Kinetics

We used the total nutrient spiraling curves to fit spiraling parameters to a MM kinetic model (Covino et al., 2010; Newbold et al., 2006). Even though these relationships are useful to characterize the stream response to the variable nutrient concentration, accurate estimation of ambient metrics from tracer additions represent a significant challenge (Rodriguez-Cardona et al., 2016). As we expected due to the scale of our columns, the extrapolated ambient uptake lengths found were between 10 and 10,000 times shorter than values reported in the literature (Covino et al., 2012; Wollheim et al., 2014; Trentman et al. 2014; Gibson et al., 2015; Rodriguez-Cardona et al., 2016). However, U_{amb} and V_{f-add} were in some cases comparable to metrics found in headwater studies (Covino et al., 2010,2012; Rodriguez-Cardona et al., 2016; Piper et al., 2017).

Total uptake velocity decreased with $NO_3 - N_{total}$, generally following MM kinetics. This suggests that our systems reached uptake saturation and were consistent with the behaviors reported in the literature for streams (Mulholland et al., 2008; Covino et al., 2010,2012; Wollheim et al., 2014; Trentman et al. 2014; Gibson et al., 2015; Rodriguez-Cardona et al., 2016; Piper et al., 2017). The magnitudes observed for K_s and U_{max} were similar to the kinetic parameters found in headwater nutrient additions (Covino et al., 2012; Wollheim et al., 2014; Piper et al., 2017). Among the different substrates, the relationships found for silica sand showed lack of relationship between V_{f-tot} and nutrient concentration, indicating that rate of nutrient loss is proportional to the concentration of nutrient.

Besides the widely accepted MM nutrient spiraling correlation, during two experiments we observed a positive correlation between uptake velocity and nutrient concentration

(V_{f-tot} increased with$NO_3 - N_{total}$). Day and Hall, (2017) observed this behavior during short-term ammonium additions in headwater streams and adopted the term "efficiency gain" to describe the model. Diemer et al. (2015) also observed this pattern after nutrient additions across sites with a wide range of wildfire burn histories. They explained this behavior using the biostimulation model, which describes the increased nutrient demand with concentration as a result of adsorption, luxury uptake, or storage above that which occurs during normal equilibrium conditions. Moreover, Rodríguez-Cardona et al. (2016) also observed this kinetic response in streams with high and low ambient NO_3 concentrations. They attributed this response to a potential fertilization effect in streams caused by large additions of the nutrient. Although our columns only presented this pattern in 1st and 2nd order silica for the nitrate experiments, it was only statistically significant ($p<0.05$) for the 2nd order stream.

NO_3-N uptake and stoichiometric limitations along the continuum

We observed higher uptake velocity curves with increasing concentrations during the Redfield injection in 17 of the 24 comparisons (Figures 6 and 7). In general, for native sediments, Ks values were lower in nitrate experiments and U_{max} increased during the Redfield experiment, however the opposite pattern was observed for gravel (Table 11). The combination of results obtained for uptake curves and kinetics suggest that NO_3-N processing along our river continuum was limited by N and co-limited by P and C, and that the efficiency of NO_3-N uptake is enhanced with the availability of limiting nutrients. Due to the strong relationship between nutrient supply and biomass growth, short-term nutrient additions can be used as a proxy to understand potential nutrient limitations of

the microorganisms along the continuum (Piper et al., 2017). Enhanced NO_3-N removal during Redfield experiments suggests P and C co-limitation. However, if nitrate uptake remained invariable across experiments (or slightly decreased from nitrate to Redfield experiments), the system could be considered only N limited.

In summary, we used consistent column experiments with sediments from across a 1st to 8th order river continuum and varied nutrient supply (only nitrate vs Redfield or stoichiometrically 'balanced' additions) to understand how nitrate uptake varies across space and under ideal resource supply conditions. Our results support the concept that stoichiometrically balanced nutrient supply enhances nutrient uptake. Even though interactions between limiting nutrients have been most frequently studied by ecologists working with phytoplankton, our results are consistent with their findings. Fracoeur, (2001) conducted a meta-analysis of lotic studies and found that algae were more likely to be limited by both N and P. Tank and Dodds, (2003) found similar results while testing autotrophic (algae) and heterotrophic (fungi) nutrient limitation across 10 North American streams in nutrient diffusing agar devices. Their results also indicated that P limitation alone was unlikely despite the low concentrations of the nutrient found in most of the streams under evaluation. Dodds et al. (2004) found that nitrate uptake in aquatic ecosystems was linked to carbon availability, suggesting that N retention decreases as C:N ratios decrease. Piper et al. (2017), assed N and P co-limitation using short term nutrient additions in 3 oligotrophic mountain streams and found that uptake of N and P were strongly enhanced in the presence of the other nutrient.

Table 11. Comparison NO_3-N uptake parameters derived from Michaelis-Menten in nitrate and Redfield experiments by stream order and sediment texture. N corresponds to comparisons where at least one of the experiments exhibited kinetic parameters far from saturation.

	Native						Gravel						Silica					
	MM Umax (µg m^{-2} min^{-1})			MM Ks (µg L^{-1})			MM Umax (µg m^{-2} min^{-1})			MM Ks (µg L^{-1})			MM Umax (µg m^{-2} min^{-1})			MM Ks (µg L^{-1})		
Stream order	Nitrate	Redfield		Nitrate	Redfield		Nitrate	Redfield		Nitrate	Redfield		Nitrate	Redfield		Nitrate	Redfield	
1st	136	149	↑	2371	4098	↑	6.5E+5	20	**N**	692	8.9E+7	**N**	4.8E+6	177	**N**	9.2E+8	20610	**N**
2nd	47	65	↑	3082	1140	↓	19	127	↑	10098	1082	↓	4.3E+7	28	**N**	5.5E+9	1413	**N**
3rd	67	87	↑	1307	100	↓	132	30	↓	281	5981	↑	179	125	↓	7407	3995	↓
4th	30	6.6E+6	**N**	805	7.3E+8	**N**	99	32	↓	837	5012	↑	1.7E+06	82	**N**	1.4E+8	2693	**N**
5th	78	149	↑	2742	5255	↑	1231	157	↓	4663	79141	↑	1008	4207	↑	45255	255400	↑
7th_A	65	205	↑	1491	1742	↑	68	16	↓	250	3568	↑	698	53	↓	67953	2743	↓
7th_B	70	52	↓	383	134	↓	4.7E+6	50	**N**	636	9.7E+8	**N**	71	1193	↑	14573	162212	↑
8th	38	69	↑	192	198	↑	8	28	↑	50	198	↑	18	1.2E+6	**N**	1895	1.4E+8	**N**

CONCLUSION

Our column experiments using sediments from across a 1st to 8th order river continuum and varying nutrient supply (only nitrate vs Redfield or stoichiometrically 'balanced' additions) suggest that solute-specific nitrate uptake metrics cannot be easily scaled along the continuum. Nutrients were processed more efficiently in columns packed with native sediments, potentially due to enhanced physical and chemical characteristics that increased biomass diversity and density. Our comparison of NO_3-N uptake metrics for nitrate and Redfield experiments suggested that nitrate uptake is enhanced by the availability of carbon and phosphorous, supporting cell-scale results previously observed. Our results suggest that traditional solute-specific analyses hinder scaling patterns of nutrient uptake dynamics and call for stoichiometrically focused investigations that, at the minimum, consider C, N and P dynamics. Because we did not track C and P concentrations along with NO_3 and conservative tracer concentrations, we could not resolve the scaling relationship of nutrient uptake across a river continuum. Therefore, we suggest that upcoming investigations of nutrient transport and export across rivers and watersheds should integrate a stoichiometric component.

ACKNOWLEDGEMENTS

We acknowledge Jacob Mortensen, Cameron Herrington, Betsy Summers and James Fluke for lab and field assistance. Funding for this project was provided by New Mexico Water Resources Research Institute and the National Science Foundation the Center for Water and the Environment (HRD-1345169).

APPENDIX

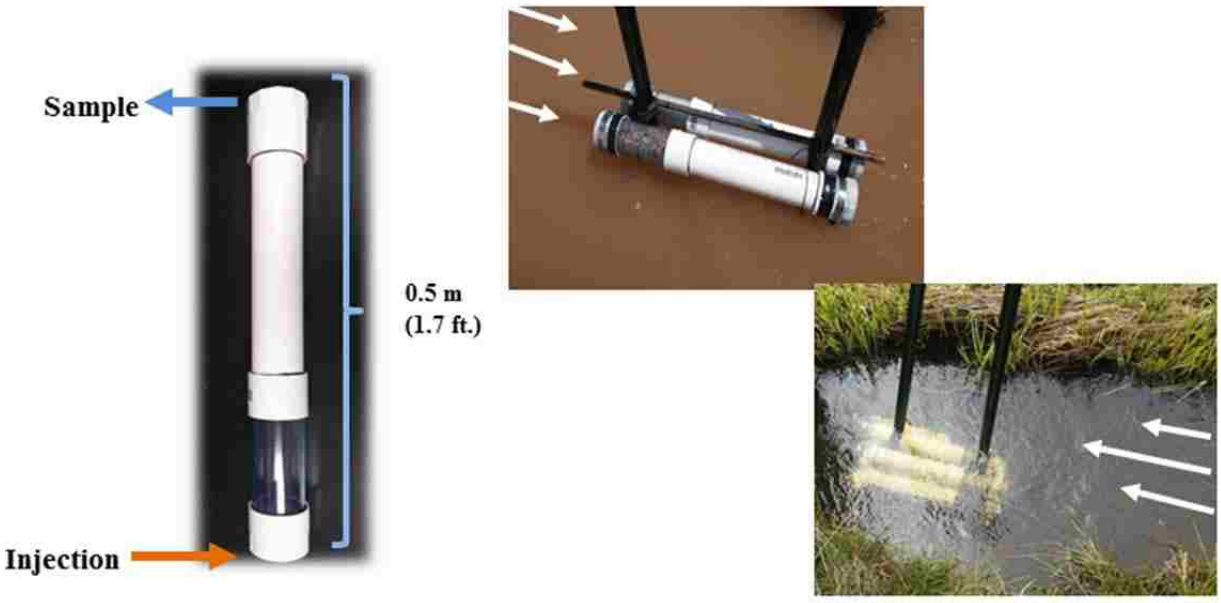

Figure S1. (a) Mescosm design and sampling port. (b) Incubation configuration.

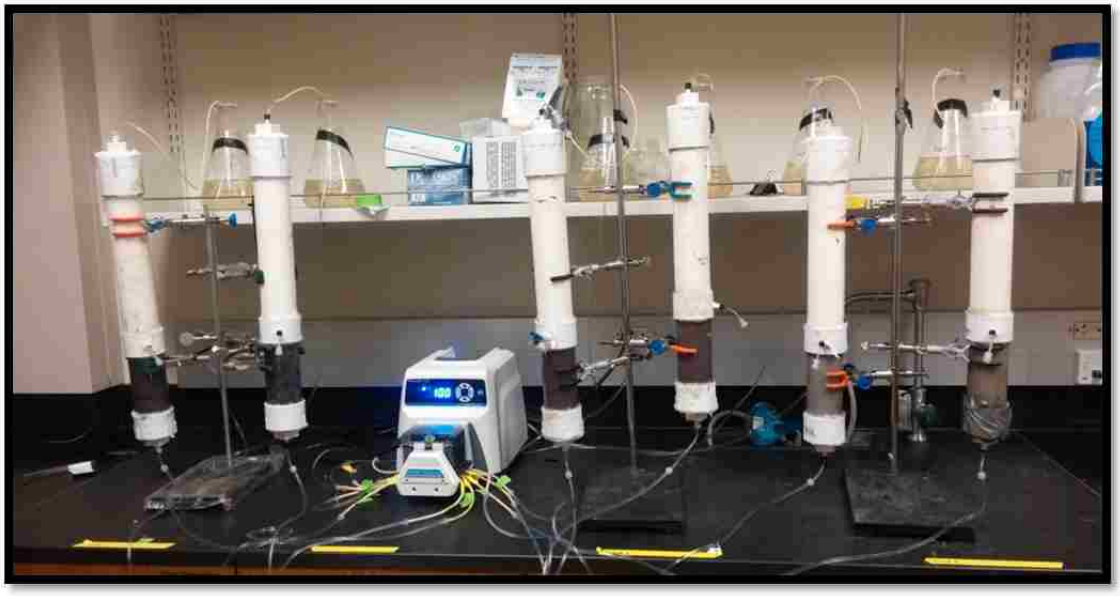

Figure S2. Experimental setup. Six PVC columns packed in two replicates with three different materials 1) gravel, 2) native sediments, and 3) silica sand.

Table S1. Summary of uptake metrics found for nitrate experiments. Mean, median, minimum and maximum of each spiraling metric by stream order and substrate. Last column presents a summary of the metrics observed for each stream order in different sediment textures, while the last row corresponds to a summary of the metrics explored for all stream orders within the same sediment texture.

	Native			Gravel			Silica sand			All Substrates		
Stream order	**Sw_{add} (m)**	**Vf_{add}(mm min^{-1})**	**U_{add} (µg m^{-2} min^{-1})**	**Sw_{add} (m)**	**Vf_{add}(mm min^{-1})**	**U_{add} (µg m^{-2} min^{-1})**	**Sw_{add} (m)**	**Vf_{add}(mm min^{-1})**	**U_{add} (µg m^{-2} min^{-1})**	**Sw_{add} (m)**	**Vf_{add}(mm min^{-1})**	**U_{add} (µg m^{-2} min^{-1})**
1st	1.19	0.05	46.95	4.33	0.007	8.76	8.74	0.01	14.71	4.48	0.02	23.10
	1.22	0.03	54.23	4.34	0.007	9.20	5.73	0.006	15.11	4.25	0.01	14.18
	0.14-2.4	0.013-0.224	5.4-64.8	3.7-4.8	0.007-0.009	2.5-16.7	2.6-26.6	0.001-0.012	0.3-37.0	0.1-26.6	0.001-0.224	0.3-64.8
2nd	2.91	0.01	11.17	4.82	0.008	7.50	12.34	0.01	31.06	6.10	0.01	15.33
	2.94	0.01	8.37	4.48	0.007	6.20	3.20	0.010	12.69	3.14	0.01	8.24
	1.6-4.4	0.007-0.020	0.6-25.4	1.8-10.3	0.003-0.018	1.6-20.4	2.2-54.6	0.001-0.015	0.04-93.9	1.6-54.6	5.83E-04-0.020	0.04-93.9
3rd	1.38	0.04	22.51	1.74	0.019	19.83	1.63	0.02	30.52	1.59	0.02	24.13
	1.33	0.02	18.96	1.78	0.018	20.73	1.73	0.018	24.60	1.78	0.02	20.52
	0.2-2.2	0.014-0.155	2.4-49.6	1.4-2.0	0.016-0.023	7.0-30.6	1.0-1.9	0.016-0.069	3.5-69.0	0.2-2.2	0.014-0.155	2.4-69.0
4th	2.08	0.02	16.56	2.02	0.017	16.45	2.63	0.012	26.63	2.20	0.02	19.17
	2.22	0.01	17.25	2.09	0.015	17.15	2.67	0.012	24.94	2.27	0.01	17.90
	0.3-2.8	0.011-0.102	4.0-25.7	1.0-2.6	0.012-0.031	3.2-34.0	1.5-3.1	0.010-0.031	0.5-49.5	0.3-3.1	0.010-0.102	0.5-49.5
5th	2.28	0.02	35.48	2.13	0.015	38.82	1.62	0.02	113.51	2.08	0.02	53.24
	2.04	0.02	34.65	2.11	0.015	41.58	1.64	0.019	124.82	1.99	0.02	40.82
	0.4-3.5	0.009-0.083	5.6-83.3	1.8-2.6	0.012-0.018	6.6-75.8	1.3-1.8	0.017-0.025	8.2-227.8	0.4-3.5	0.009-0.083	5.6-227.8
7th_A	1.61	0.02	31.80	2.55	0.014	20.20	3.25	0.01	28.11	2.36	0.02	26.89
	1.89	0.02	33.28	2.86	0.011	17.62	3.24	0.010	27.79	2.53	0.01	26.56
	0.6-2.1	0.015-0.100	3.5-62.4	1.0-3.6	0.009-0.031	3.9-41.1	2.8-3,8	0.008-0.017	4.5-53.1	0.6-3.8	0.008-0.055	3.5-62.4
7th_B	1.94	0.02	24.99	7.24	0.005	13.78	10.60	0.004	12.65	5.96	0.01	17.73
	2.14	0.01	22.98	5.50	0.006	14.41	9.81	0.003	11.34	4.53	0.007	20.38
	0.4-3.1	0.010-0.089	13.6-36.8	4.3-14.1	0.002-0.007	0.6-26.3	3.5-19.4	0.002-0.009	3.9-23.1	0.4-19.4	0.002-0.089	0.6-36.8
8th	1.29	0.04	20.28	5.27	0.012	5.46	6.92	0.007	8.55	4.07	0.02	11.77
	1.26	0.02	20.99	5.34	0.006	4.14	6.64	0.005	8.33	2.56	0.01	10.87
	0.2-2.6	0.012-0.197	6.8-30.8	0.5-11.7	0.003-0.061	1.5-13.4	1.3-11.5	0.003-0.025	1.0-18.4	0.2-11.7	0.003-0.197	1.0-30.8
All stream orders	1.82	0.03	25.05	3.58	0.01	16.97	5.88	0.01	28.54			
	1.91	0.02	21.85	2.35	0.01	11.64	3.20	0.01	17.34			
	0.1-4.4	0.007-0.224	0.6-83.3	0.4-14.1	0.002-0.071	0.6-75.8	1.0-54.6	0.001-0.032	0.04-227.8			

Table S2. Summary of uptake metrics found for Redfield experiments. Mean, median, minimum and maximum of each spiraling metric by stream order and substrate. Last column presents a summary of the metrics observed for each stream order in different sediment textures, while the last row corresponds to a summary of the metrics explored for all stream orders within the same sediment texture.

	Native			Gravel			Silica sand			All Substrates		
Stream order	Sw_{add} (m)	Vf_{add}(mm min^{-1})	U_{add} (µg m^{-2} min^{-1})	Sw_{add} (m)	Vf_{add}(mm min^{-1})	U_{add} (µg m^{-2} min^{-1})	Sw_{add} (m)	Vf_{add}(mm min^{-1})	U_{add} (µg m^{-2} min^{-1})	Sw_{add} (m)	Vf_{add}(mm min^{-1})	U_{add} (µg m^{-2} min^{-1})
1st	1.41	0.03	25.86	2.48	0.017	8.02	7.84	0.01	34.37	2.48	0.02	20.19
	1.51	0.02	16.41	2.51	0.013	6.38	4.43	0.007	23.12	2.02	0.02	9.76
	0.3-2.2	0.014-0.112	1.9-87.8	0.7-4.0	0.008-0.046	1.5-36.9	0.4-7.8	0.004-0.086	1.9-151.3	0.3-7.8	0.004-0.112	1.5-151.3
2nd	1.50	0.05	20.00	3.54	0.020	9.45	5.10	0.02	40.09	3.15	0.03	22.02
	1.34	0.02	22.62	3.00	0.011	7.62	5.90	0.005	13.87	2.15	0.01	11.89
	0.13-4.4	0.007-0.250	0.3-34.7	0.3-11.0	0.003-0.124	0.9-41.5	0.3-12	0.003-0.121	0.2-264.6	0.1-12.0	0.003-0.250	0.2-264.6
3rd	1.07	0.07	26.11	1.32	0.038	16.49	1.62	0.02	41.55	1.30	0.04	26.04
	1.33	0.03	25.20	1.40	0.023	16.71	1.72	0.019	45.79	1.40	0.02	22.43
	0.1-2.2	0.015-0.406	1.8-66.3	0.2-2.3	0.014-0.145	4.5-27.1	0.9-2.1	0.015-0.035	9.5-67.7	0.1-2.3	0.014-0.406	1.8-67.7
4th	4.82	0.01	11.63	1.83	0.026	12.00	1.86	0.032	32.14	2.93	0.02	17.30
	2.22	0.01	7.28	2.16	0.015	9.22	1.86	0.017	22.17	2.27	0.01	10.97
	0.7-14.2	0.002-0.048	0.4-35.1	0.3-3.4	0.009-0.094	1.8-35.8	0.3-4.1	0.008-0.120	1.5-156.8	0.3-14.2	0.002-0.120	0.4-156.8
5th	2.08	0.02	50.86	1.34	0.045	44.86	3.03	0.015	71.22	1.94	0.03	47.96
	2.04	0.01	46.87	1.44	0.022	55.94	2.04	0.016	64.39	2.06	0.02	46.13
	0.7-3.0	0.011-0.047	4.1-100.1	0.2-2.4	0.013-0.195	3.9-69.9	1.8-3.0	0.011-0.018	0.8-172.2	0.2-4.2	0.008-0.196	0.8-172.2
7th_A	0.55	0.07	83.73	3.43	0.022	9.96	4.07	0.01	22.35	2.60	0.04	39.64
	0.63	0.05	88.30	3.78	0.008	10.57	3.63	0.009	20.69	1.79	0.02	19.53
	0.2-0.7	0.043-0.161	13.6-127.1	0.2-6.2	0.005-0.136	2.7-15.7	0.7-9.3	0.003-0.048	1.8-45.1	0.2-9.3	0.003-0.161	1.8-127.1
7th_B	0.62	0.06	49.95	1.21	0.034	28.32	7.25	0.01	18.28	1.75	0.04	33.89
	0.64	0.05	57.95	1.31	0.024	29.67	4.36	0.007	15.60	1.08	0.030	32.24
	0.2-0.9	0.035-0.167	11.8-68.9	0.3-1.8	0.018-0.111	6.8-48.4	3.1-7.3	0.004-0.010	1.6-44.8	0.2-7.3	0.004-0.167	1.6-68.9
8th	1.90	0.02	16.48	1.23	0.040	12.40	3.69	0.01	17.44	2.04	0.03	14.83
	1.60	0.02	16.41	1.03	0.032	10.66	3.53	0.009	18.30	1.88	0.02	15.94
	0.4-3.4	0.009-0.086	7.8-35.8	0.3-2.3	0.014-0.111	4.1-22.2	3.0-4.7	0.007-0.131	2.0-30.8	0.2-4.7	0.007-0.111	3.3-35.8
All stream orders	1.82	0.04	32.78	1.78	0.03	18.24	3.52	0.02	31.50			
	1.37	0.02	22.77	1.50	0.02	14.07	3.22	0.01	19.53			
	0.1-14.2	0.002-0.406	0.3-127.1	0.2-6.2	0.005-0.195	1.1-69.9	0.3-12.0	0.003-0.121	0.2-256.6			

REFERENCES

Alexander, R. B., Smith, R. A., and Schwarz, G. E. "Effect of Stream Channel Size on the Delivery of Nitrogen to the Gulf of Mexico" *Nature* 403, no. 6771 (2000): 758–761. doi:10.1038/35001562

Allgeier, J. E., Rosemond, A. D., and Layman, C. A. "Variation in Nutrient Limitation and Seagrass Nutrient Content in Bahamian Tidal Creek Ecosystems" *Journal of Experimental Marine Biology and Ecology* 407, no. 2 (2011): 330–336. doi:10.1016/j.jembe.2011.07.005

Appling, A. P. and Heffernan, J. B. "Nutrient Limitation and Physiology Mediate the Fine-Scale (De)coupling of Biogeochemical Cycles" *The American Naturalist* 184, no. 3 (2014): 384–406. doi:10.1086/677282

Bardini, L., Boano, F., Cardenas, M. B., Revelli, R., and Ridolfi, L. "Nutrient Cycling in Bedform Induced Hyporheic Zones" *Geochimica et Cosmochimica Acta* 84, (2012): 47–61. doi:10.1016/j.gca.2012.01.025

Bernhardt, E. S., Likens, G. E., Buso, D. C., and Driscoll, C. T. "In-Stream Uptake Dampens Effects of Major Forest Disturbance on Watershed Nitrogen Export" *Proceedings of the National Academy of Sciences* 100, no. 18 (2003): 10304–10308. doi:10.1073/pnas.1233676100

Bekins, B. A., Warren, E., and Godsy, E. M. "A Comparison of Zero-Order, First-Order, and Monod Biotransformation Models" *Ground Water* 36, no. 2 (1998): 261–268. doi:10.1111/j.1745-6584.1998.tb01091.x

Boano, F., Demaria, A., Revelli, R., and Ridolfi, L. "Biogeochemical Zonation due to Intrameander Hyporheic Flow" *Water Resources Research* 46, no. 2 (2010): W02511. doi:10.1029/2008WR007583

Brookshire, E. N. J., Valett, H. M., Thomas, S. A., and Webster, J. R. "Coupled Cycling of Dissolved Organic Nitrogen and Carbon in a Forest Stream" *Ecology* 86, no. 9 (2005): 2487–2496. doi:10.1890/04-1184

Cohen, M. J., Kurz, M. J., Heffernan, J. B., Martin, J. B., Douglass, R. L., Foster, C. R., and Thomas, R. G. "Diel Phosphorus Variation and the Stoichiometry of Ecosystem Metabolism in a Large Spring-Fed River" *Ecological Monographs* 83, no. 2 (2013): 155–176. doi:10.1890/12-1497.1

Craigg, S. D. "Hydrologic Data on the Pueblos of Jemez, Zia, and Santa Ana, Sandoval County, New Mexico" (1984): Available at http://pubs.er.usgs.gov/publication/ofr84460

Covino, T. P., McGlynn, B. L., and McNamara, R. A. "Tracer Additions for Spiraling Curve Characterization (TASCC): Quantifying Stream Nutrient Uptake Kinetics from Ambient to Saturation" *Limnology and Oceanography: Methods* 8, no. 9 (2010): 484–498. doi:10.4319/lom.2010.8.484

Covino, T., McGlynn, B., and McNamara, R. "Land Use/Land Cover and Scale Influences on in-Stream Nitrogen Uptake Kinetics" *Journal of Geophysical Research: Biogeosciences* 117, no. G2 (2012): G02006. doi:10.1029/2011JG001874

Dahm, C. N., Candelaria-Ley, R. I., Reale, C. S., Reale, J. K., and Van Horn, D. J. "Extreme Water Quality Degradation Following a Catastrophic Forest Fire" *Freshwater Biology* 60, no. 12 (2015): 2584–2599. doi:10.1111/fwb.12548

Davis, J. C. and Minshall, G. W. “Nitrogen and Phosphorus Uptake in Two Idaho (USA) Headwater Wilderness Streams” *Oecologia* 119, no. 2 (1999): 247–255. doi:10.1007/s004420050783

Day, N. K. and Hall, R. O. “Ammonium Uptake Kinetics and Nitrification in Mountain Streams” *Freshwater Science* 36, no. 1 (2017): 41–54. doi:10.1086/690600

Dodds, W. K., Martí, E., Tank, J. L., Pontius, J., Hamilton, S. K., Grimm, N. B., Bowden, W. B., McDowell, W. H., Peterson, B. J., Valett, H. M., Webster, J. R., and Gregory, S. “Carbon and Nitrogen Stoichiometry and Nitrogen Cycling Rates in Streams” *Oecologia* 140, no. 3 (2004): 458–467. doi:10.1007/s00442-004-1599-y

Earl, S. R., Valett, H. M., and Webster, J. R. “Nitrogen Saturation in Stream Ecosystems” *Ecology* 87, no. 12 (2006): 3140–3151. doi:10.1890/0012-9658(2006)87[3140:NSISE]2.0.CO;2

Elser, J. J., Bracken, M. E. S., Cleland, E. E., Gruner, D. S., Harpole, W. S., Hillebrand, H., Ngai, J. T., Seabloom, E. W., Shurin, J. B., and Smith, J. E. “Global Analysis of Nitrogen and Phosphorus Limitation of Primary Producers in Freshwater, Marine and Terrestrial Ecosystems” *Ecology Letters* 10, no. 12 (2007): 1135–1142. doi:10.1111/j.1461-0248.2007.01113.x

Elser, J. J., Andersen, T., Baron, J. S., Bergström, A.-K., Jansson, M., Kyle, M., Nydick, K. R., Steger, L., and Hessen, D. O. “Shifts in Lake N:P Stoichiometry and Nutrient Limitation Driven by Atmospheric Nitrogen Deposition” *Science* 326, no. 5954 (2009): 835–837. doi:10.1126/science.1176199

Ensign, S. H. and Doyle, M. W. "Nutrient Spiraling in Streams and River Networks" *Journal of Geophysical Research: Biogeosciences* 111, no. G4 (2006): G04009. doi:10.1029/2005JG000114

Figueroa-Nieves, D., McDowell, W. H., Potter, J. D., and Martínez, G. "Limited Uptake of Nutrient Input from Sewage Effluent in a Tropical Landscape" *Freshwater Science* 35, no. 1 (2015): 12–24. doi:10.1086/684992

Fisher, S. G., Sponseller, R. A., and Heffernan, J. B. "Horizons in Stream Biogeochemistry: Flowpaths to Progress" *Ecology* 85, no. 9 (2004): 2369–2379. doi:10.1890/03-0244

Francoeur, S. N. "Meta-Analysis of Lotic Nutrient Amendment Experiments: Detecting and Quantifying Subtle Responses" *Journal of the North American Benthological Society* 20, no. 3 (2001): 358–368. doi:10.2307/1468034

Gibson, C. A. and O'Reilly, C. M. "Organic Matter Stoichiometry Influences Nitrogen and Phosphorus Uptake in a Headwater Stream" *Freshwater Science* 31, no. 2 (2012): 395–407. doi:10.1899/11-033.1

Gibson, C. A., O'Reilly, C. M., Conine, A. L., and Lipshutz, S. M. "Nutrient Uptake Dynamics across a Gradient of Nutrient Concentrations and Ratios at the Landscape Scale" *Journal of Geophysical Research: Biogeosciences* 120, no. 2 (2015): 2014JG002747. doi:10.1002/2014JG002747

Gomez, J. D., Wilson, J. L., and Cardenas, M. B. "Residence Time Distributions in Sinuosity-Driven Hyporheic Zones and Their Biogeochemical Effects" *Water Resources Research* 48, no. 9 (2012): W09533. doi:10.1029/2012WR012180

González-Pinzón, R., Mortensen, J., and Van Horn, D. "Comment on 'Solute-Specific Scaling of Inorganic Nitrogen and Phosphorus Uptake in Streams' by Hall et Al. (2013)" *Biogeosciences* 12, no. 18 (2015): 5365–5369. doi:10.5194/bg-12-5365-2015

Hendricks, S. P. "Microbial Ecology of the Hyporheic Zone: A Perspective Integrating Hydrology and Biology" *Journal of the North American Benthological Society* 12, no. 1 (1993): 70–78. doi:10.2307/1467687

Hall Jr., R. O., Baker, M. A., Rosi-Marshall, E. J., Tank, J. L., and Newbold, J. D. "Solute-Specific Scaling of Inorganic Nitrogen and Phosphorus Uptake in Streams" *Biogeosciences* 10, no. 11 (2013): 7323–7331. doi:10.5194/bg-10-7323-2013

Hill, B. H., McCormick, F. H., Harvey, B. C., Johnson, S. L., Warren, M. L., and Elonen, C. M. ; "Microbial Enzyme Activity, Nutrient Uptake and Nutrient Limitation in Forested Streams" *Freshwater Biology* 55, (2010): 1005–1019.

Hall, R. J. O., Bernhardt, E. S., and Likens, G. E. "Relating Nutrient Uptake with Transient Storage in Forested Mountain Streams" *Limnology and Oceanography* 47, no. 1 (2002): 255–265. doi:10.4319/lo.2002.47.1.0255

Hecky, R. E., Campbell, P., and Hendzel, L. L. "The Stoichiometry of Carbon, Nitrogen, and Phosphorus in Particulate Matter of Lakes and Oceans" *Limnology and Oceanography* 38, no. 4 (1993): 709–724. doi:10.4319/lo.1993.38.4.0709

Harpole, W. S., Ngai, J. T., Cleland, E. E., Seabloom, E. W., Borer, E. T., Bracken, M. E. S., Elser, J. J., Gruner, D. S., Hillebrand, H., Shurin, J. B., and Smith, J. E. "Nutrient Co-Limitation of Primary Producer Communities" *Ecology Letters* 14, no. 9 (2011): 852–862. doi:10.1111/j.1461-0248.2011.01651.x

Hall, R., Baker, M., Arp, C., and Koch, B. “Hydrologic Control of Nitrogenremoval, Storage and Export in a Mountain Stream” *Limnology and Oceanography* (2009): 2128–2142.

Harvey, J. W., Böhlke, J. K., Voytek, M. A., Scott, D., and Tobias, C. R. “Hyporheic Zone Denitrification: Controls on Effective Reaction Depth and Contribution to Whole-Stream Mass Balance” *Water Resources Research* 49, no. 10 (2013): 6298–6316. doi:10.1002/wrcr.20492

Kiel, B. A. and Bayani Cardenas, M. “Lateral Hyporheic Exchange throughout the Mississippi River Network” *Nature Geoscience* 7, no. 6 (2014): 413–417. doi:10.1038/ngeo2157

Knapp, J. L. A., González-Pinzón, R., Drummond, J. D., Larsen, L. G., Cirpka, O. A., and Harvey, J. W. “Tracer-Based Characterization of Hyporheic Exchange and Benthic Biolayers in Streams” *Water Resources Research* 53, no. 2 (2017): 1575–1594. doi:10.1002/2016WR019393

Klausmeier, C. A., Litchman, E., Daufresne, T., and Levin, S. A. “Optimal Nitrogen-to-Phosphorus Stoichiometry of Phytoplankton” *Nature* 429, no. 6988 (2004): 171–174. doi:10.1038/nature02454

Marklein, A. R. and Houlton, B. Z. “Nitrogen Inputs Accelerate Phosphorus Cycling Rates across a Wide Variety of Terrestrial Ecosystems” *The New Phytologist* 193, no. 3 (2012): 696–704. doi:10.1111/j.1469-8137.2011.03967.x

Marzadri, A., Tonina, D., and Bellin, A. "A Semianalytical Three-Dimensional Process-Based Model for Hyporheic Nitrogen Dynamics in Gravel Bed Rivers" *Water Resources Research* 47, no. 11 (2011): W11518. doi:10.1029/2011WR010583

Mortensen, J. G., González-Pinzón, R., Dahm, C. N., Wang, J., Zeglin, L. H., and Van Horn, D. J. "Advancing the Food-Energy–Water Nexus: Closing Nutrient Loops in Arid River Corridors" *Environmental Science & Technology* 50, no. 16 (2016): 8485–8496. doi:10.1021/acs.est.6b01351

Mulholland, P. J., Helton, A. M., Poole, G. C., Hall, R. O., Hamilton, S. K., Peterson, B. J., Tank, J. L., Ashkenas, L. R., Cooper, L. W., Dahm, C. N., Dodds, W. K., Findlay, S. E. G., Gregory, S. V., Grimm, N. B., Johnson, S. L., McDowell, W. H., Meyer, J. L., Valett, H. M., Webster, J. R., Arango, C. P., Beaulieu, J. J., Bernot, M. J., Burgin, A. J., Crenshaw, C. L., Johnson, L. T., Niederlehner, B. R., O'Brien, J. M., Potter, J. D., Sheibley, R. W., Sobota, D. J., and Thomas, S. M. "Stream Denitrification across Biomes and Its Response to Anthropogenic Nitrate Loading" *Nature* 452, no. 7184 (2008): 202–205. doi:10.1038/nature06686

Mulholland, P. J., Hall, R. O., Sobota, D. J., Dodds, W. K., Findlay, S. E. G., Grimm, N. B., Hamilton, S. K., McDowell, W. H., O'Brien, J. M., Tank, J. L., Ashkenas, L. R., Cooper, L. W., Dahm, C. N., Gregory, S. V., Johnson, S. L., Meyer, J. L., Peterson, B. J., Poole, G. C., Valett, H. M., Webster, J. R., Arango, C. P., Beaulieu, J. J., Bernot, M. J., Burgin, A. J., Crenshaw, C. L., Helton, A. M., Johnson, L. T., Niederlehner, B. R., Potter, J. D., Sheibley, R. W., and Thomasn, S. M. "Nitrate Removal in Stream Ecosystems Measured by 15N Addition Experiments: Denitrification" *Limnology and Oceanography* 54, no. 3 (2009): 666–680. doi:10.4319/lo.2009.54.3.0666

Mulholland, P. J., Tank, J. L., Webster, J. R., Bowden, W. B., Dodds, W. K., Gregory, S. V., Grimm, N. B., Hamilton, S. K., Johnson, S. L., Martí, E., McDowell, W. H., Merriam, J. L., Meyer, J. L., Peterson, B. J., Valett, H. M., and Wollheim, W. M. "Can Uptake Length in Streams Be Determined by Nutrient Addition Experiments? Results from an Interbiome Comparison Study" *Journal of the North American Benthological Society* 21, no. 4 (2002): 544–560. doi:10.2307/1468429

Newbold, J. D., Elwood, J. W., O'Neill, R. V., and Sheldon, A. L. "Phosphorus Dynamics in a Woodland Stream Ecosystem: A Study of Nutrient Spiralling" *Ecology* 64, no. 5 (1983): 1249–1265. doi:10.2307/1937833

Newbold, J. D., Bott, T. L., Kaplan, L. A., Dow, C. L., Jackson, J. K., Aufdenkampe, A. K., Martin, L. A., Horn, D. J. V., and Long, A. A. "Uptake of Nutrients and Organic C in Streams in New York City Drinking-Water-Supply Watersheds" *Journal of the North American Benthological Society* 25, no. 4 (2006): 998–1017. doi:10.1899/0887-3593(2006)025[0998:UONAOC]2.0.CO;2

Navel, S., Mermillod-Blondin, F., Montuelle, B., Chauvet, E., Simon, L., and Marmonier, P. "Water–Sediment Exchanges Control Microbial Processes Associated with Leaf Litter Degradation in the Hyporheic Zone: A Microcosm Study" *Microbial Ecology* 61, no. 4 (2011): 968–979. doi:10.1007/s00248-010-9774-7

O'Brien, J. M., Dodds, W. K., Wilson, K. C., Murdock, J. N., and Eichmiller, J. "The Saturation of N Cycling in Central Plains Streams: 15N Experiments across a Broad Gradient of Nitrate Concentrations" *Biogeochemistry* 84, no. 1 (2007): 31–49. doi:10.1007/s10533-007-9073-7

Oelsner, G. P., Brooks, P. D., and Hogan, J. F. "Nitrogen Sources and Sinks Within the Middle Rio Grande, New Mexico1" *JAWRA Journal of the American Water Resources Association* 43, no. 4 (2007): 850–863. doi:10.1111/j.1752-1688.2007.00071.x

Parmenter, R. R., Steffen, A., and Allen, C. D. "An Overview of the Valles Caldera National Preserve: The Natural and Cultural Resources" (2007): 147–154. Available at https://pubs.er.usgs.gov/publication/70176090

Passell, H. D., Dahm, C. N., and Bedrick, E. J. "Hydrological and Geochemical Trends and Patterns in the Upper Rio Grande, 1975 to 19991" *JAWRA Journal of the American Water Resources Association* 40, no. 1 (2004): 111–127. doi:10.1111/j.1752-1688.2004.tb01014.x

Piper, L. R., Cross, W. F., and McGlynn, B. L. "Colimitation and the Coupling of N and P Uptake Kinetics in Oligotrophic Mountain Streams" *Biogeochemistry* 132, no. 1–2 (2017): 165–184. doi:10.1007/s10533-017-0294-0

Payn, R. A., Webster, J. R., Mulholland, P. J., Valett, H. M., and Dodds, W. K. "Estimation of Stream Nutrient Uptake from Nutrient Addition Experiments: Estimation of Stream Nutrient Uptake" *Limnology and Oceanography: Methods* 3, no. 3 (2005): 174–182. doi:10.4319/lom.2005.3.174

Poole, G. C., O'Daniel, S. J., Jones, K. L., Woessner, W. W., Bernhardt, E. S., Helton, A. M., Stanford, J. A., Boer, B. R., and Beechie, T. J. "Hydrologic Spiralling: The Role of Multiple Interactive Flow Paths in Stream Ecosystems" *River Research and Applications* 24, no. 7 (2008): 1018–1031. doi:10.1002/rra.1099

Pinay, G., O'Keefe, T. C., Edwards, R. T., and Naiman, R. J. "Nitrate Removal in the Hyporheic Zone of a Salmon River in Alaska" *River Research and Applications* 25, no. 4 (2009): 367–375. doi:10.1002/rra.1164

Redfield, A. C. "The Biological Control of Chemical Factors in the Environment" *American scientist* 46, no. 3 (1958): 230A–221.

Rodríguez-Cardona, B., Wymore, A. S., and McDowell, W. H. "DOC:NO3− Ratios and NO3− Uptake in Forested Headwater Streams" *Journal of Geophysical Research: Biogeosciences* 121, no. 1 (2016): 2015JG003146. doi:10.1002/2015JG003146

Reale, J. K., Van Horn, D. J., Condon, K. E., and Dahm, C. N. "The Effects of Catastrophic Wildfire on Water Quality along a River Continuum" *Freshwater Science* 34, no. 4 (2015): 1426–1442. doi:10.1086/684001

Ribot, M., Von Schiller, D., Peipoch, M., Sabater, F., Grimm, N. B., and Martí, E. "Influence of Nitrate and Ammonium Availability on Uptake Kinetics of Stream Biofilms" *Freshwater Science* 32, no. 4 (2013): 1155–1167.

Schade, J. D., MacNEILL, K., Thomas, S. A., CAMILLE McNEELY, F., Welter, J. R., Hood, J., Goodrich, M., Power, M. E., and Finlay, J. C. "The Stoichiometry of Nitrogen and Phosphorus Spiralling in Heterotrophic and Autotrophic Streams" *Freshwater Biology* 56, no. 3 (2011): 424–436. doi:10.1111/j.1365-2427.2010.02509.x

Tank, J. L. and Dodds, W. K. "Nutrient Limitation of Epilithic and Epixylic Biofilms in Ten North American Streams" *Freshwater Biology* 48, no. 6 (2003): 1031–1049. doi:10.1046/j.1365-2427.2003.01067.x

Trentman, M. T., Dodds, W. K., Fencl, J. S., Gerber, K., Guarneri, J., Hitchman, S. M., Peterson, Z., and Rüegg, J. "Quantifying Ambient Nitrogen Uptake and Functional

Relationships of Uptake versus Concentration in Streams: A Comparison of Stable Isotope, Pulse, and Plateau Approaches" *Biogeochemistry* 125, no. 1 (2015): 65–79. doi:10.1007/s10533-015-0112-5

Tank, J. L., Rosi-Marshall, E. J., Baker, M. A., and Hall, R. O. "Are Rivers Just Big Streams? A Pulse Method to Quantify Nitrogen Demand in a Large River" *Ecology* 89, no. 10 (2008): 2935–2945. doi:10.1890/07-1315.1

Valett, H. M., Morrice, J. A., Dahm, C. N., and Campana, M. E. "Parent Lithology, Surface–groundwater Exchange, and Nitrate Retention in Headwater Streams" *Limnology and Oceanography* 41, no. 2 (1996): 333–345. doi:10.4319/lo.1996.41.2.0333

Wollheim, W. M., Harms, T. K., Peterson, B. J., Morkeski, K., Hopkinson, C. S., Stewart, R. J., Gooseff, M. N., and Briggs, M. A. "Nitrate Uptake Dynamics of Surface Transient Storage in Stream Channels and Fluvial Wetlands" *Biogeochemistry* 120, no. 1–3 (2014): 239–257. doi:10.1007/s10533-014-9993-y

Webster, J. R., Mulholland, P. J., Tank, J. L., Valett, H. M., Dodds, W. K., Peterson, B. J., Bowden, W. B., Dahm, C. N., Findlay, S., Gregory, S. V., Grimm, N. B., Hamilton, S. K., Johnson, S. L., Martí, E., Mcdowell, W. H., Meyer, J. L., Morrall, D. D., Thomas, S. A., and Wollheim, W. M. "Factors Affecting Ammonium Uptake in Streams – an Inter-Biome Perspective" *Freshwater Biology* 48, no. 8 (2003): 1329–1352. doi:10.1046/j.1365-2427.2003.01094.x

Workshop, S. S. "Concepts and Methods for Assessing Solute Dynamics in Stream Ecosystems" *Journal of the North American Benthological Society* 9, no. 2 (1990): 95–119. doi:10.2307/1467445

Wondzell, S. M. "The Role of the Hyporheic Zone across Stream Networks" *Hydrological Processes* 25, no. 22 (2011): 3525–3532. doi:10.1002/hyp.8119

Zarnetske, J. P., Haggerty, R., Wondzell, S. M., and Baker, M. A. "Dynamics of Nitrate Production and Removal as a Function of Residence Time in the Hyporheic Zone" *Journal of Geophysical Research: Biogeosciences* 116, no. G1 (2011): G01025. doi:10.1029/2010JG001356

Zarnetske, J. P., Haggerty, R., Wondzell, S. M., Bokil, V. A., and González-Pinzón, R. "Coupled Transport and Reaction Kinetics Control the Nitrate Source-Sink Function of Hyporheic Zones" *Water Resources Research* 48, no. 11 (2012): W11508. doi:10.1029/2012WR011894

Zeglin, L. H. "Stream Microbial Diversity in Response to Environmental Changes: Review and Synthesis of Existing Research" *Frontiers in Microbiology* 6, (2015): doi:10.3389/fmicb.2015.00454